

Disclaimer

The ABCB and the Participating Governments are committed to enhancing the availability and dissemination of information relevant to the built environment. A Fatigue Damage to Metal Battens Subjected to Simulated Wind Loads (the Report) is designed in making such information easily available. However neither the ABCB, the Participating Governments, nor the groups or individuals which have been involved in the development of the Report, accept any responsibility for the use of the information contained in the Report and make no warranty or representation whatsoever that the information is an exhaustive treatment of the subject matters contained therein or is complete, accurate, up-to-date or relevant as a guide to action for any particular purpose. Users are required to exercise their own skill and care with respect to its use. In any important matter, users should carefully evaluate the scope of the treatment of the particular subject matter, its completeness, accuracy, currency and relevance for their purposes, and should obtain appropriate professional advice relevant to the particular circumstances.

In particular, and to avoid doubt, the use of the Report does not:

- guarantee acceptance or accreditation of a material by any entity authorised to do so under any law;
- mean that a material complies with the BCA; or
- absolve the user from complying with any State, Territory or Commonwealth regulatory requirements.

The ABCB does not hold any responsibility for the accessibility of the Report or related documents under Web Content Accessibility Guidelines (WCAG 2.0).

JAMES COOK UNIVERSITY

SCHOOL OF ENGINEERING

EG4010

Civil Engineering

**FATIGUE DAMAGE TO METAL BATTENS
SUBJECTED TO SIMULATED WIND LOADS**

Rebecca Fowler

**Thesis submitted to the School of Engineering in partial fulfilment of the
requirements for the degree of**

Bachelor of Civil Engineering with Honours

06/09/03

ABSTRACT

The traditional 40mm deep timber roof batten is increasingly being replaced by the thin gauge steel “top-hat” batten in domestic house roof systems. Extensive research has been conducted on roof cladding since the cyclones of the 1970’s, which found that low-cycle fatigue was a major cause of damage. The batten-truss connection experiences large wind loads similar to the cladding and there is concern that the battens may be susceptible to low-cycle fatigue. The objective of this thesis is to study the fatigue performance of the battens using analysis methods applied in studying cladding fatigue. A series of tensile tests, static tests, constant amplitude cyclic tests and block cyclic load tests were conducted and the results obtained provided information for the fundamental understanding of the battens fatigue behaviour.

The tests conducted in determining the fatigue behaviour of the batten were carried out on the INSTRON (model 1342) universal testing machine with a capacity of 100kN, in the structures lab at the School of Engineering, James Cook University. A testing apparatus was designed so that static and cyclic loads could be applied to the batten-truss connection. Two battens were chosen for the investigation the Stramit Cyclonic Roof batten and the BHP Topspan 40 batten. Both battens had different geometries and were specified for cyclonic areas. Static test results obtained an average static failure load for each batten which was used to determine the upper cyclic load bound for the constant amplitude cyclic tests. A series of constant amplitude cyclic tests were conducted at different load levels to obtain an S-N curve. Constant amplitude cyclic tests were discontinued on the BHP batten as there were difficulties simulating the batten hold down used in industry. Block cyclic load tests conducted on the Stramit batten revealed that Miner’s rule could be used as a preliminary estimate of the damage caused to the batten.

Tensile test results determined that the 0.75 bmt G550 material used in the battens had a tensile strength of approximately 650MPa. Static test results obtained an average static failure load of 8.95kN for the Stramit batten with a standard deviation of 0.57kN. The BHP batten had an average static failure load of 7.56kN with a standard deviation of 0.83kN. These average static failure loads were determined to be at least twice that of the specified design loads. Results from the batten tests were compared with

findings from previous studies on cladding to determine if there were any similarities in the fatigue behaviour. Studies on cladding has found that the S-N curve is segmented unlike that of the Stramit batten which was determined to have an S-N curve that can be closely approximated by a straight line. Both cladding and the Stramit batten showed crack patterns that are associated with different load levels. The cladding having four different crack patterns associated with four different load levels and the Stramit batten having four crack patterns associated with two different load levels.

Theoretical analysis of testing regimes and simulated wind events were applied to the Stramit batten and results have determined that it is likely to withstand an 8 hour strong wind event. It was also determined that the batten's hold down conditions (i.e. initial tightness of the fastener) affected the fatigue behaviour. Information from these investigations will benefit the thin-gauge steel top hat batten manufacturing industry and the building industry by providing the foundations for understanding the fatigue behaviour of battens.

STATEMENT ON SOURCES DECLARATION

I declare that this thesis is my own work and has not been submitted in any form for another degree or diploma at any university or other institution of tertiary education. Information derived from the published or unpublished work of others has been acknowledged in the text and a list of references is given.

Rebecca Fowler

Date

STATEMENT OF ACCESS

I, the undersigned, the author of this thesis, understand that James Cook University will make available for the use within the University Library and, by microfilm or other means, allow access to other users in other approved libraries. All users consulting this thesis will have to sign the following statement:

In consulting this thesis I agree not to copy or closely paraphrase it in whole or in part without the written consent of the author, and to make proper public written acknowledgement for any assistance, which I have obtained from it.

Beyond this, I do not wish to place any restriction on access to this thesis.

Rebecca Fowler

Date

ACKNOWLEDGEMENTS

This thesis was conducted under the supervision of Dr John Ginger, Lecturer at James Cook University and Research Director of the Cyclone Testing Station and Mr David Henderson, Manager of the Cyclone Testing Station. With sincere gratitude I would like to thank John and David their assistance and guidance throughout the duration of this thesis.

Thanks are also extended to Mr Curt Arrowsmith for manufacturing the testing apparatus; Mr Stu Petersen for his excellent technical guidance with the testing equipment and Mr Don Braddick for this assistance with the preparation of the testing specimens and help during the testing.

Finally thank-you to my parents and family for there continued support and encouragement throughout the years.

CONTENTS

TOPIC	PAGE
Title Page	i
Abstract	ii
Statement of Sources	iv
Statement of Access	v
Acknowledgments	vi
Contents	vii
List of Tables	x
List of Figures	xi
Notations	xii
Chapter 1 Introduction	1
Chapter 2 Literature Review	5
2.1 Fatigue	5
2.1.1 S – N Curve	5
2.1.2 Miner’s Rule	8
2.2 Fatigue Testing Regimes	9
2.2.1 DABM (1976)	9
2.2.2 Melbourne (1977)	9
2.2.3 TR440 (1978)	10
2.2.4 Beck and Stevens (1979)	10
2.2.5 Random Block Loading (RBL) (1990)	10
2.2.6 LHL (1993)	10
2.3 Design Loads	11
2.4 Rainflow Count Method	12
2.5 Fatigue Life under Wind Loading	13
2.6 Fatigue of Cladding and its Fixings	14
2.6.1 Material	14
2.6.2 Fatigue Performance	15

CONTENTS

TOPIC	PAGE
Chapter 3 Experimental Method	18
3.1 Test Configuration	19
3.2 Tensile Tests	21
3.3 Static Tests	22
3.4 Constant Amplitude Cyclic Tests	22
3.5 Block Cyclic Load Tests	23
Chapter 4 Experimental Results, Discussion and Analysis	24
4.1 Tensile Tests	24
4.2 Static Tests	25
4.2.1 BHP Topspan 40 Batten	25
4.2.2 Stramit Cyclonic Roof Batten	27
4.3 Constant Amplitude Cyclic Tests	30
4.3.1 BHP Topspan 40 Batten	30
4.3.2 Stramit Cyclonic Roof Batten	31
4.4 Block Loads	36
4.4.1 Stramit Cyclonic Roof Batten	36
4.5 Application of Loading Regimes	39
4.6 Fatigue Behaviour under Wind Loading	40
4.7 Narrow Band and Wide Band Damage	43
4.8 Cladding Fatigue vs. Batten Fatigue	44
Chapter 5 Conclusions and Recommendations	48
5.1 Conclusions	49
5.2 Recommendations	50
References	52
APPENDIX A Batten Specifications and Design Capacity Tables	54
APPENDIX B INSTRON Calibration	60

CONTENTS

TOPIC	PAGE
APPENDIX C Tensile Test Results	62
APPENDIX D Summary of Static Test Results	64
APPENDIX E Load vs. Displacement curves for Static Tests	69
APPENDIX F Stramit Constant Amplitude Test Results	75
APPENDIX G Observed Crack Initiation and Propagation for 80% and 70% Constant Amplitude Cyclic Tests	77

LIST OF TABLES

	PAGE
Table 4.1 Tensile test results	24
Table 4.2 BHP Batten failure loads	26
Table 4.3 Stramit batten failure loads	29
Table 4.4 Constant amplitude test results for BHP batten	30
Table 4.5 Constant amplitude test results for Stramit batten	31
Table 4.6 Crack types at different load levels	35
Table 4.7 Block load test results	37
Table 4.8 Critical damage coefficient	39
Table 4.9 Batten behaviour under TR440	40
Table 4.10 Batten behaviour under L-H-L	40
Table 4.11 Batten behaviour under DABM	40
Table 4.12 Area B Net Cps [10]	41
Table 4.13 Batten behaviour under pressure measurement from the Texas Tech building	43

LIST OF FIGURES

	PAGE
Figure 1.1 Typical domestic house roof system	2
Figure 2.1 Form of typical S-N curve	6
Figure 2.2 Form of a typical S-N curve when log S is plotted against log N	6
Figure 2.3 Cycling about zero mean	7
Figure 2.4 Cycling about a specified nonzero mean	7
Figure 2.5 Cycling between zero and S_{max}	7
Figure 2.6 Low–High–Low loading regime	11
Figure 2.7 Areas on the roof and wall subjected to high pressures with a local pressure factor of $k_1 = 2$	12
Figure 2.8 Narrow band random vibrations [13]	13
Figure 2.9 Wide band random vibrations [13]	13
Figure 2.10 Common cladding profiles [24]	14
Figure 2.11 Crack patterns from constant amplitude cyclic loading [11]	16
Figure 2.12 S-N curve for corrugated cladding fastened without cyclone washers [15]	17
Figure 3.1 Cross-section of Stramit Cyclonic Roof batten	18
Figure 3.2 Cross-section of BHP Topspan 40 batten	18
Figure 3.3 Test Setup	20
Figure 3.4 Schematic of testing apparatus (not to scale)	20
Figure 3.5 Batten screw (12 gauge) and washer used in laboratory experiments	21
Figure 3.6 Tensile test dimensions (not to scale)	22
Figure 4.1 BHP Static Test load vs. displacement curve	25
Figure 4.2 BHP batten static failure mode at narrow turned over edge	26
Figure 4.3 BHP batten static failure mode at the unsymmetric wider turned over edge	27
Figure 4.4 Type 1 Stramit static test load vs. displacement curve	28
Figure 4.5 Type 2 Stramit static test load vs. displacement curve	28
Figure 4.6 Stramit Batten failure mode	29
Figure 4.7 Stramit Batten failure mode	29
Figure 4.8 S-N curve for Stramit Cyclonic Roof batten	32
Figure 4.9 N-S curve for the Stramit batten	33

LIST OF FIGURES

	PAGE
Figure 4.10 Type A	34
Figure 4.11 Type B	34
Figure 4.12 Type C	34
Figure 4.13 Type D	34
Figure 4.14 Batten failure in Cyclone Testing Station air-box test	36
Figure 4.15 Batten failure in Cyclone Testing Station air-box test	36
Figure 4.16 13.7 × 9.1 × 4.0 m full-scale Texas Tech building showing cladding-fastener tributary area A (1.0 × 0.2 m ²) and batten-truss tributary area B (1.0 × 1.8 m ²) [10]	41

NOTATIONS

a	= function of the exponent m
b	= function of the exponent m
bmt	= base metal thickness
$C_{p,e}$	= external pressure coefficient
$C_{p,i}$	= internal pressure coefficient
$C_{p,n}$	= net pressure coefficient
D	= wide band random stress damage
D_{nb}	= narrow band stress damage
d	= depth
h	= height
K	= constant depending on material properties
k_l	= local pressure factor
M	= exponent also depending on material properties varies between 5 and 20
m_k	= k th moment of the spectral density
N	= number of cycles to failure
n	= number of stress cycles at an amplitude
p_{net}	= net design wind pressure
R	= stress ratio
S	= stress amplitude
S_{max}	= upper stress bound
S_{min}	= lower stress bound
$V_{des,?}$	= building orthogonal design wind speeds
w	= width
e	= spectral bandwidth parameter
$?$	= parameter determined empirically
ρ_{air}	= density of air (1.2kg/m^3)

Chapter 1 Introduction

Domestic houses can sustain damage during extreme windstorms such as cyclones and thunderstorms. The roofing system experiences large wind loads and components such as the cladding and battens are susceptible to severe damage. Extensive research has been conducted on roof cladding since the cyclones of the 1970's, which found that low-cycle fatigue was a major cause of damage. The fluctuating wind loads during a cyclone produce high stress concentrations around the fastener head causing fatigue cracking. Under continued loading the cracks propagate until the cladding pulls over the fastener. This increases the load on the adjacent fastener resulting in progressive failure of the roof system. Comprehensive research and testing on roof systems have provided workable solutions to minimise these failures by the inclusion of cyclone washers in conjunction with cladding fasteners. Testing regimes have also been developed to simulate extreme wind events that the roofing systems are evaluated against.

Wind loads have a fluctuating nature, and continued cycling accumulates damage that leads to fatigue failure. Low-cycle fatigue failure is where a structure fails at loads lower than the static failure load over several hundred to several thousand cycles. Simplified testing regimes have been developed to evaluate cladding as the fluctuating nature of the wind loads are very complex to simulate. The DABM (Darwin Area Building Manual) testing regime was introduced by the Darwin Reconstruction committee after cyclone Tracy in 1974 and incorporated into the Northern Territory Appendix of the Building Code of Australia [7]. This testing regime was considered to be too conservative and TR440 [22] was developed. TR440 has been widely accepted in cyclone prone areas of Australia, except in the Northern Territory where the DABM test regime continues to be applied. TR440 has been incorporated into AS4040.3 [5] and AS1170.2 (1989) [2], however removed from AS/NZS 1170.2 (2002) [3]. A number of studies have been conducted on the validity of these testing regimes and the Low – High - Low (LHL) method has been proposed. Though testing methods and studies have been primarily concentrated on cladding, the code specifications indicate that they should be used to evaluate the cladding and its immediate fixings, which includes the batten-truss connection. In testing the

fatigue performance of the batten, analysis methods used in studying cladding fatigue will be applied. Details of these testing methods and roofing system evaluation studies are outlined Chapter 2.

The traditional 40mm deep timber battens are being increasingly replaced by thin-gauge steel “top-hat” battens. The typical low-rise domestic house roof systems in Australia consist of battens placed at about 1.0m intervals and attached to roof trusses installed up to 1.2m apart. However, the batten and truss spacing vary depending on the batten type, manufacture’s specifications and the wind classification. In these systems, the batten-truss connection has to resist wind loads acting on a tributary area of up to 1.2m^2 as shown in Figure 1.1.

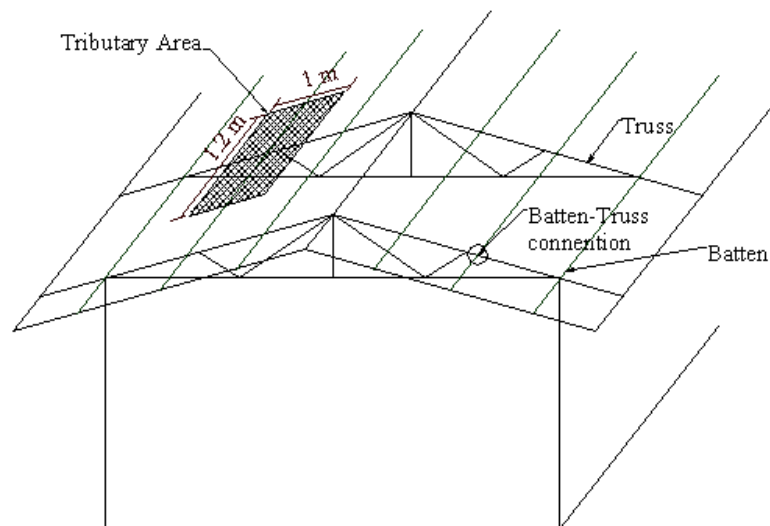


Figure 1.1 Typical domestic house roof system

The batten-truss connections can experience large wind loads near the ridge, eaves and gable end of a building and may be susceptible to low-cycle fatigue failures, similar to the fatigue behaviour at the cladding fasteners. However the effect of fluctuating loads on the batten is not always evaluated by the manufacturer. Furthermore, the change in batten material and type has also caused concern regarding the cladding to batten connection, as most research and studies were conducted using the timber battens. It has been considered that there could be problems with the cladding disengaging from the metal batten and

fastening techniques need to be explored. However the focus of this study is on the batten-truss connection.

The scope of this research is to study typical batten truss connections and determine their performance in terms of low-cycle fatigue effects. The batten-truss connection will be subjected to a series of cyclic loads and the results analysed to determine the performance of the batten subjected to wind loads. Wind loads on the connection are estimated using AS/NZS1170.2 (2002) [3] or AS4055 [6], with design loads being estimated for roof systems in cyclonic regions C and D. Typical battens used in Australia are supplied by manufacturers such as BHP and Stramit. These suppliers provide design capacity tables for each of their products, which specify batten and truss spacing as well as the design loads.

The effects of low-cycle fatigue are determined by subjecting the batten to static and cyclic loads. The static test determines the static load capacity of the batten truss connection, which is used to define the upper loading bound for the cyclic tests. A number of cyclic tests are conducted at bounds from zero to a percentage of the static failure load. The number of cycles until failure is counted and related to the S-N curve (stress amplitude vs. number of cycles). Subjecting the batten to an accumulated load history will determine if Miner's Rule can be used to predict the batten failure. The data taken from Miners Rule and the S-N curve will be applied to current testing regimes to determine the damage accumulation from these tests.

To investigate the low-cycle fatigue effect on the batten-truss connection the following aims are to be achieved:

- Identify typical battens manufactured and used in Australia, and obtain the batten spans, batten material and material thickness specifications.
- Determine the specifications of a typical batten-truss connection.
- Determine the tensile strength of batten materials.
- Determine the batten-truss connection strength under static load.

- Determine the fatigue performance of the batten- truss connection by obtaining an S-N curve.
- Subject the batten to blocks of cyclic loads at different load levels and relate the accumulated fatigue damage to Miner's rule
- Determine the damage proportion on the batten under wind loads using pressure measurements obtained from a full scale building.

A review of the procedures used to determine the fatigue behaviour of the battens and the current loading regimes are given in Chapter 2. The methodology for obtaining the experimental results and the testing apparatus set up are outlined in Chapter 3. The results from the experimental procedures and observations are documented and analysed in Chapter 4. Chapter 5 presents conclusion and recommendation from this research.

Chapter 2 Literature Review

2.1 Fatigue

Components of structures are generally subjected to fluctuating loads, also called cyclic loads, and the resulting cyclic stresses can lead to damage of the materials involved. Under continued cycling, damage accumulates which can cause cracks to develop at stresses well below the material's static strength. The process of damage and failure due to cyclic loading is called fatigue. The fatigue characteristics of a component can be determined by subjecting it to a series of cyclic loads until failure of the material. A test specimen subjected to a sufficiently severe cyclic stress, will develop fatigue cracks leading to complete failure of the specimen. If the test is carried out at a higher stress level, the number of cycles to failure will be smaller. The results from such tests of a number of different stress levels may be plotted to obtain the stress amplitude vs. number of cycles to failure curve known as the S-N curve. [8]

2.1.1 S – N Curve

In the usual failure model for the fatigue of metals it is assumed that each cycle of a sinusoidal stress response inflicts an increment of damage, which depends on the amplitude of the stress. Each successive cycle then generates additional damage which accumulates in proportion to the number of cycles until failure occurs. The results of constant amplitude fatigue tests are usually expressed in the form of an S-N curve, where S is the stress amplitude, and N is the number of cycles until failure. For many materials, the S-N curve is of the form shown in Figure 2.1. This is represented by a straight line when $\log S$ is plotted against $\log N$ as shown in Figure 2.2. This implies an equation of the form

$$NS^m = K \quad (2.1)$$

where K is a constant which depends on the material and the exponent m varies between about 5 and 20. [12], [13]

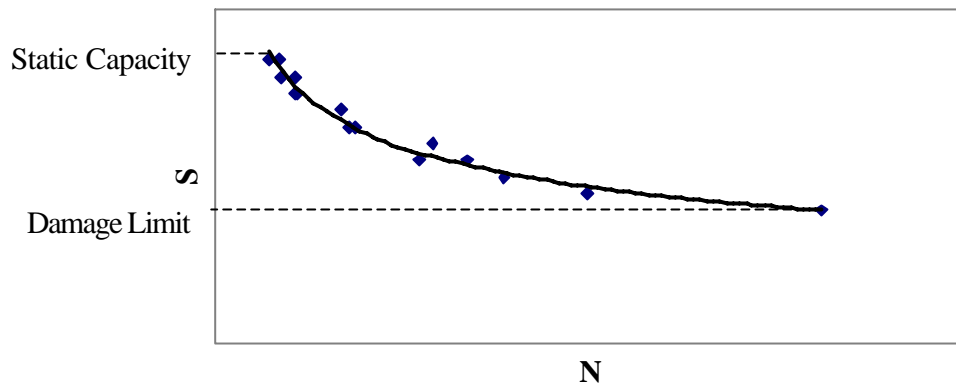


Figure 2.1 Form of typical S-N curve

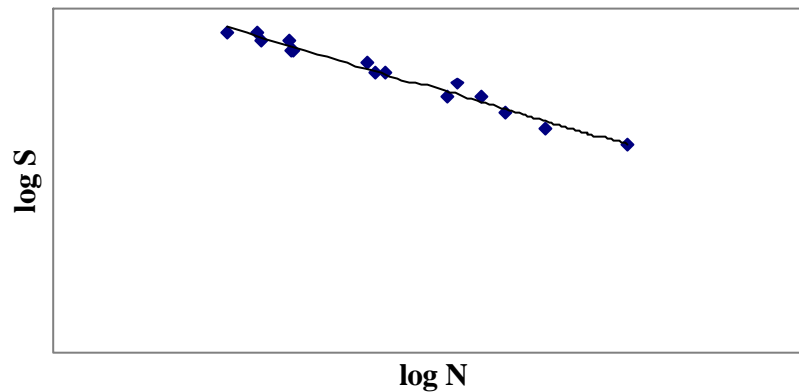


Figure 2.2 Form of a typical S-N curve when log S is plotted against log N

An S-N curve for a component can be developed by subjecting it to cyclic loads as follows:

- Cycling amplitude S , with mean of zero as shown in Figure 2.3.
- Cycling amplitude S , with a specified nonzero mean as shown in Figure 2.4
- Cycling amplitude S , with a constant stress ratio, R as shown in Figure 2.5, with $S_{\min} = 0$ and the stress ratio is

$$R = \frac{S_{\min}}{S_{\max}} \quad (2.2)$$

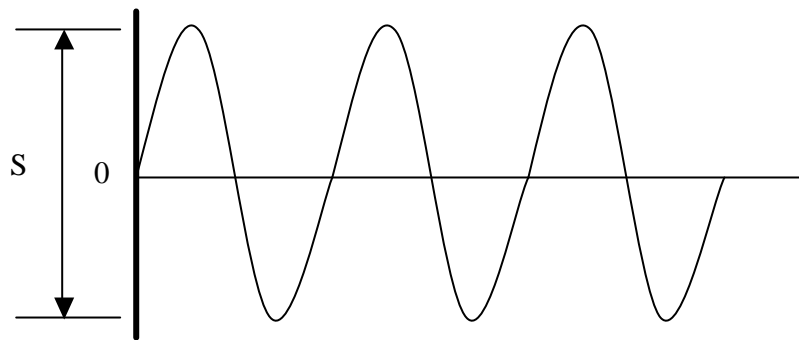


Figure 2.3 Cycling about zero mean

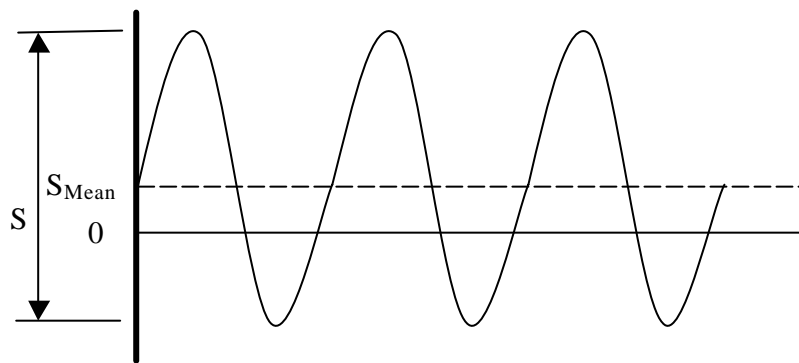


Figure 2.4 Cycling about a specified nonzero mean

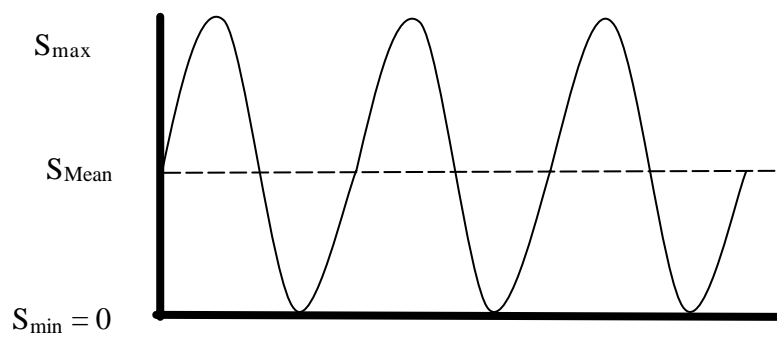


Figure 2.5 Cycling between zero and S_{\max}

The number of cycles to failure changes with stress level and may range over several orders of magnitude. For this reason, the cycle numbers are usually plotted on a logarithmic scale [8]. Another characteristics of the S-N curve is that there are typically threshold bounds, this is where failure occurs at only one cycle at a load greater than or equal to the static capacity. Furthermore, once the stress cycle is below a certain load limit the number of cycles will not have a significant damage effect on the component as shown in Figure 2.1.

2.1.2 Miner's Rule

A criterion for failure under repeated loading, with a range of different amplitudes is Miner's Rule

$$\sum \left(\frac{n_i}{N_i} \right) = 1 \quad (2.3)$$

where n_i is the number of stress cycles at an amplitude for which N_i cycles are required to cause failure. Therefore fatigue failure may occur from a very large number of low level stress cycles or from few cycles at a level near the ultimate static load capacity. There are no restrictions on the order in which the various stress amplitudes are applied in Miner's rule. Thus it may be applied to a random loading process which can be considered as a series of cycles with randomly varying amplitudes [12].

Several studies [11], [15] have shown that the application of larger load cycles early in the loading history have a significant effect on the fatigue response of the cladding than lower loads due to the changing profile properties. A decreased block load following crack initiation from a higher load, resulted in slower crack growth and longer life than if the higher block load was continued. Whereas the opposite occurred if a higher block load followed crack initiation from lower block load. A Modified Miner's rule was developed to account for the different mechanisms of fatigue damage accumulation at different load levels. However this method does not adequately predict fatigue damage, for the cladding, from cycle histories especially when higher load level cycles precede lower cycle blocks [11].

2.2 Fatigue Testing Regimes

Numerous studies have been carried out in devising loading regimes for testing and evaluating fatigue performance of roof systems [11], [16]. These testing regimes have been primarily used on cladding; however are also specified for cladding and its immediate fixing, hence applying to the batten-truss connection. Wind loads are random and fluctuating in nature and therefore difficult to incorporate in a typical lab testing regime. Many variables influence the wind loading acting on a structure, such as terrain category, roof slope, shielding, wind direction, wind speed and wind durations. These wind loads are complex and therefore must be simplified such that they can be incorporated into laboratory testing regimes. Loading regimes that have been developed to evaluate roofing products to be used in cyclonic regions of Australia include DABM and TR440, while studies have been conducted and include Melbourne, Beck and Stevers, Random Block Loading (RBL) and Low-High-Low (LHL).

2.2.1 DABM (1976)

The Darwin Reconstruction Committee implemented the cyclic load test into the Darwin Area Building Manual (DABM) in 1975. The loading criterion developed was 10,000 cycles of repeated load, varying from 0 to “permissible” design load. The permissible design load corresponded to a load derived from a 50-year return period wind speed and multiplied by a ‘cyclone multiplier’ of 1.15. Following the 10,000 cycles, the roof system is subjected to a single cycle of 0 to 1.8 times the permissible design load [16].

2.2.2 Melbourne (1977)

Melbourne (1977) developed, from wind tunnel studies, probability distributions of upcrossings of pressure fluctuations for structures oscillating under one dominant frequency. An upcrossing is the signal (pressure) exceeding a given value above a mean. The cyclic load distribution, derived from the upcrossing probability distribution is repeated three times to represent a three hour loading. The loading range of the cycles is determined by increasing standard deviations about a mean negative pressure and not just from zero load [11].

2.2.3 TR440 (1978)

The test regime specified in DABM was considered to be too conservative and the TR440 regime (a simplification of the Melbourne loading regime) was proposed. The TR440 regime consists of a three level low-high sequence, consisting of 10,200 cycles to permissible load (D), which is made up of 8000 cycles of 0-0.625D, 2000 cycles of 0-0.75D and 200 cycles of 0-1.0D, followed by an ultimate static test of 0-2D [11], [16]. This method is also included in AS1170.2 (1989) [2] and AS4040.3 [5].

2.2.4 Beck and Stevens (1979)

This loading regime was developed by analysing the pressure fluctuations from a 1/300 scale wind tunnel model study of a 10° pitch roof low-rise structure, situated in terrain category 2. A variation of the upcrossing method, called the range counting method, was used to analyse the fluctuating pressures, and convert them to cycle counts according to the magnitude and mean value of various loading fluctuations. However unlike the Melbourne sequence, only the wind suction loading was included since it was considered that only wind suction loading caused fatigue in cladding [11].

2.2.5 Random Block Loading (RBL) (1990)

The RBL regime was developed by determining pressure histories from wind tunnel studies, parametric studies of a range of wind velocities associated with Category 4 cyclones and extensive material testing of cladding. An analytical model was developed by combining all this information to formulate matrices of cycle counts of loads of varying mean and range. The rainflow counting method was used to determine the number and distribution of cycles according to the mean and range of pressure fluctuations. From the extensive matrix of loading cycles, loading blocks were randomly selected over the duration of the cyclone. Load blocks are chosen randomly during the sequence until all the load cycles in the matrix are exhausted [14], [16].

2.2.6 LHL (1993)

The Low-High-Low (LHL) method is a simplification of the complex RBL method, which was deemed too difficult and contained too many different loading levels for routine and

repeatable product evaluation. This four level, low-high-low regime, represents the loading by the passage of a cyclone, representing the wind speed increasing as the eye approaches and then decreasing as the cyclone moves way. Miner's rule was used to simplify the RBL matrix of load cycles, by comparing fatigue damage of loading blocks of similar load levels from the RBL matrix, and finding an equivalent number of cycles in the loading block of the LHL. Figure 2.6 shows the loading sequence of the LHL method where P_u is the ultimate design load [11], [14].

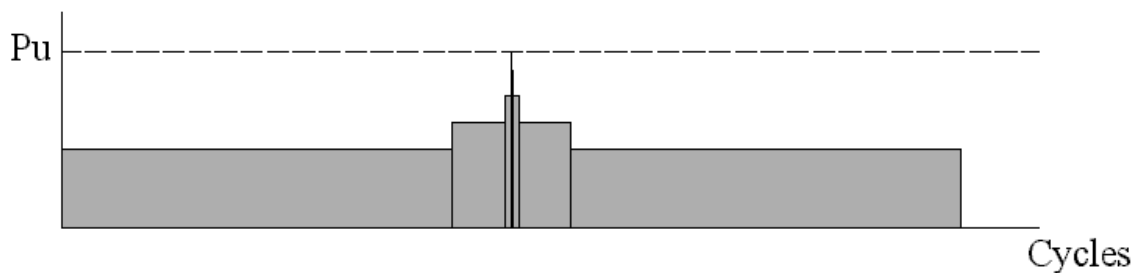


Figure 2.6 Low-High-Low loading regime

2.3 Design Loads

Many factors influence the calculation of wind loads on a roof system such as the location, terrain categories, shielding, topographic effect, building height, roof pitch and wind direction. The standards AS/NZS 1170.2 - Structural design actions, Part 2: Wind actions [3] or AS4055 - Wind loads for housing [6] can be used to calculate the wind loads on the structure and envelope. Net suction pressures on cladding and its fixings are the highest near the gable end of a roof and the edge of a low pitched roof as shown in Figure 2.7. For example a building 5m high in cyclonic region C with a terrain category of 2.5

gives $V_{des,q} = 60.6m/s$. Internal and external pressure coefficients are dependent on the building geometry and the roof pitch. The maximum external pressure coefficient for a roof is $(C_{p,e}) = -0.9$. Local pressure factors for the roof edge and gable is $(k_1) = 2$ giving a factored external pressure coefficient $(C_{p,e}) = -1.8$. The internal pressure coefficient $(C_{p,i}) = 0.7$, and combined with the external pressure coefficient gives a net pressure coefficient $(C_{p,n}) = -2.5$. From this the net design pressure of the roof is calculated

by $p_{net} = C_{p,n} \cdot 0.5 \rho_{air} V_{des,q}^2$, where $V_{des,q} = 60.6m/s$, resulting in a net pressure of 5.5 kPa.

This pressure acts over a tributary area of approximately $1.2m^2$ giving a load of 6.6kN.

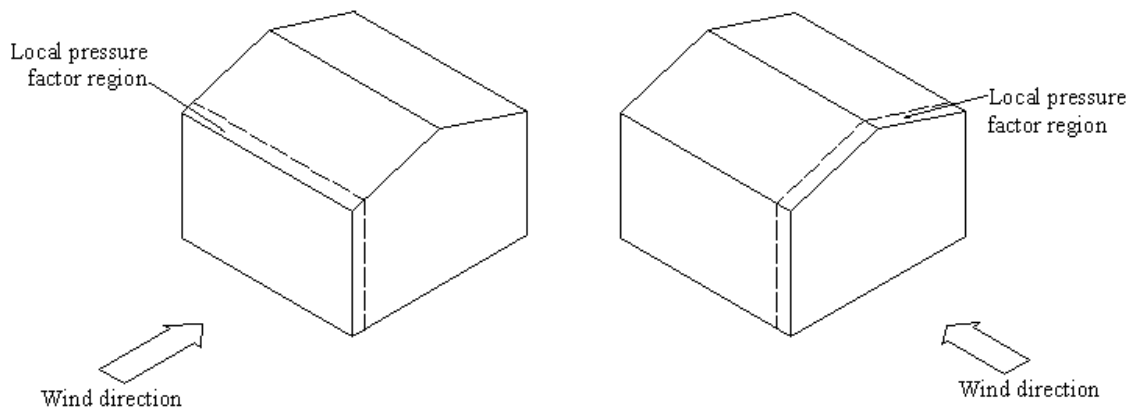


Figure 2.7 Areas on the roof and wall subjected to high pressures with a local pressure factor of $k_1 = 2$

2.4 Rainflow Count Method

Wind pressures are highly fluctuating and random and are difficult to simulate. In order to carry out a fatigue analysis on the batten truss connection it is required that the number of cycles can be counted and the period of time in which they occur can be determined. There are a number of statistical methods which enable the number of cycles to be counted, the most appropriate being the rainflow count method [1]. The rainflow method is a cycle-counting technique that enables the simplification of complex loading sequences in a form suitable for fatigue analysis of structures, such as fatigue life prediction and simulation testing. Rainflow counting results allows a reconstruction of a possibly different sequence which contains exactly the same cycles as the original sequence. This method also gives the mean value and the peak to peak range of each cycle, and provides a count of the cycles within nominated means and ranges [1].

Cycles of pressure determined using the rainflow count method, have been extracted from pressure measurements on the 13.7 (w) x 9.1 (d) x 4.0 (h) m full-scale Texas Tech building. Findings showed that the batten-truss connection is subjected to the similar number of cycles as the cladding however, loads are of a lower magnitude [10].

2.5 Fatigue Life under Wind Loading

The variable nature of wind loading produces fluctuating stresses in structures with contributions from resonant and background (sub-resonant) components. For most structures wide band background contribution is usually the dominant source of fatigue damage. Some wind loading situations produce resonant narrow-band vibrations as shown in Figure 2.8. Wide band random vibrations consists of contributions over a broad range of frequencies, with large background response peaks, this type of response is typical for wind loading, as shown in Figure 2.9.

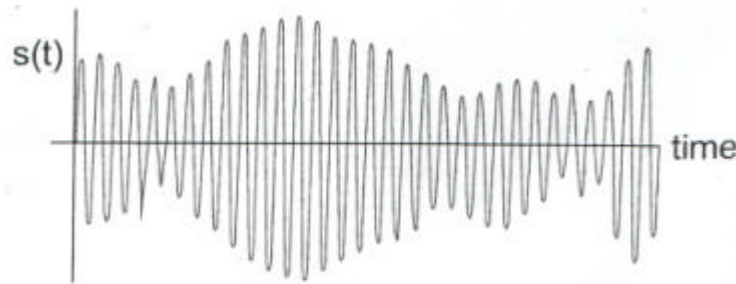


Figure 2.8 Narrow band random vibrations [13]

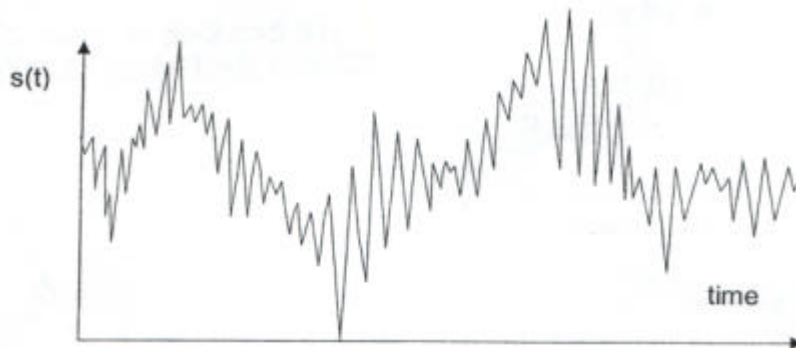


Figure 2.9 Wide band random vibrations [13]

A number of cycle counting methods for wide band stress variations have been proposed, with the rainflow count method considered the most appropriate. The fractional fatigue damage D under wide band random stress variation can be written as:

$$D = \alpha D_{nb} \quad (2.4)$$

where, D_{nb} is the damage calculated for narrow band vibration with the same standard deviation as the wide band vibrations. α is a parameter determined empirically. The

approach used to determine Δ is to use simulations of wide band processes with spectral densities of various shapes and band-widths, and rainflow counting for fatigue cycles. The formula to estimate Δ is:

$$I = a + (1 - a)(1 - e)^b \quad (2.5)$$

where a and b are functions of the exponent m from the Equation 2.1

$$a \cong 0.926 - 0.033m \quad (2.6)$$

$$b \cong 1.587m - 2.323 \quad (2.7)$$

e is the spectral bandwidth parameter equal to:

$$e = 1 - \frac{m_2^2}{m_0 m_4} \quad (2.8)$$

where m_k is the k th moment of the spectral density defined by:

$$m_k = \int_0^{\infty} f^k S(f) df \quad (2.9)$$

For narrow band vibration e tends to zero and Δ approaches 1. As e tends to its maximum possible value of 1, Δ approaches a . These values enable upper and lower limits on the damage to be determined [13].

2.6 Fatigue of Cladding and its Fixings

2.6.1 Material

The most common light gauge metal cladding used in domestic roofing is of the corrugated or rib/pan profiles, and is rolled from 0.42mm bmt G550 coil. The measured mean yield stress typically exceeds 700MPa, satisfying the minimum yield stress for G550 of 550MPa. The mechanical properties vary in the longitudinal and transverse directions of the coil. Three common pierce fixed profiles are shown in Figure 2.10.



(a) Corrugated Type

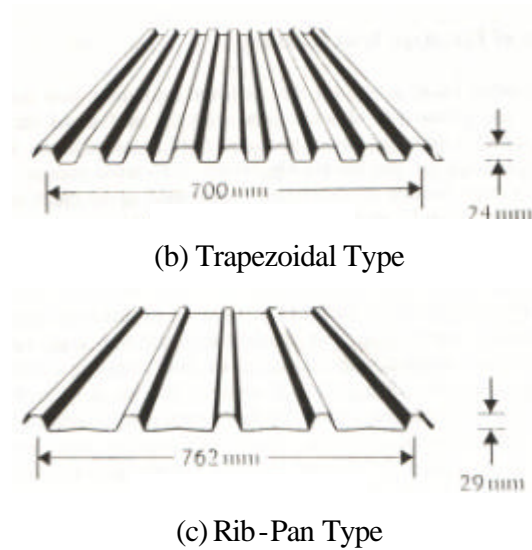


Figure 2.10 Common cladding profiles [24]

2.6.2 Fatigue Performance

The fatigue behaviour of the cladding is dependent on the load causing local plastic deformation (LPD), seen as dimpling under the screws around the fastener holes. The LPD strength strongly influences the fatigue life. The resistance to fatigue of the cladding increases noticeably if the cyclic load per fastener is kept below the LPD load. It was noted that there is a progressive reduction in the strength of the cladding-fastener assembly under repeated loading and the number of cycles to failure increases as the load per fastener decreases [11].

The fatigue resistance of the corrugated cladding at low amplitude block loading is higher than that of the rib-pan and trapezoidal cladding, but under high amplitude loading the situation is reversed. Studies have found that the cladding profile does affect the mechanism of fatigue damage accumulation. Laboratory studies have also showed that a decreased block load, following crack initiation from a higher block load, resulted in slower crack growth and longer life than if the higher block load was continued. Whereas rapid crack growth was observed, decreasing the cladding life when an increased load was applied after crack initiation from a lower block load.

From extensive constant amplitude cyclic load tests for the corrugated profile, different crack propagation modes were observed for cycling at different load levels. Sample data collected in laboratory experiments showed the variable nature of fatigue of claddings, which is not just limited to the variation in material properties across the coil, but also includes tightness, alignment and position of the screw on the crest or rib. Figure 2.11 shows the different modes of crack initiation and propagation indicative of different fatigue responses depending on the load levels. Figure 2.12 shows the S-N curve for corrugated cladding fastened without cyclone washers. For the constant amplitude load tests, when the load per cycle is well below the LPD load of 600N, cracks propagated from the screw hole along the crest (Type B in Figure 2.11 and Segment 1 in Figure 2.12). When the load per cycle is around 500N per fastener (approaching LPD) cracks propagate in both longitudinal and transverse directions (Type A-B in Figure 2.11 and approaching Segment 2 from Segment 1 in Figure 2.12). For loads cycling through the LPD cracks initiated at the edges of the flattened crests where the cladding creases, with the cracks then progressing towards the screw hole and failure within 1000 cycles (Type A in Figure 2.11 and Segment 2 in Figure 2.12). The Type C failure is from a few cycles at high loads, not unlike a straight static pull through failure [11], [15], [23] and [24].

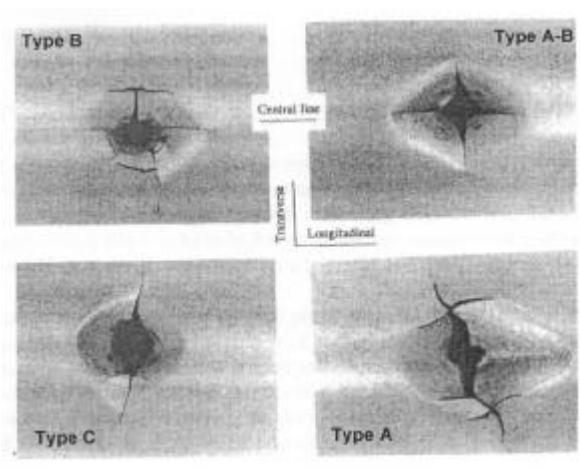


Figure 2.11 Crack patterns from constant amplitude cyclic loading [11]

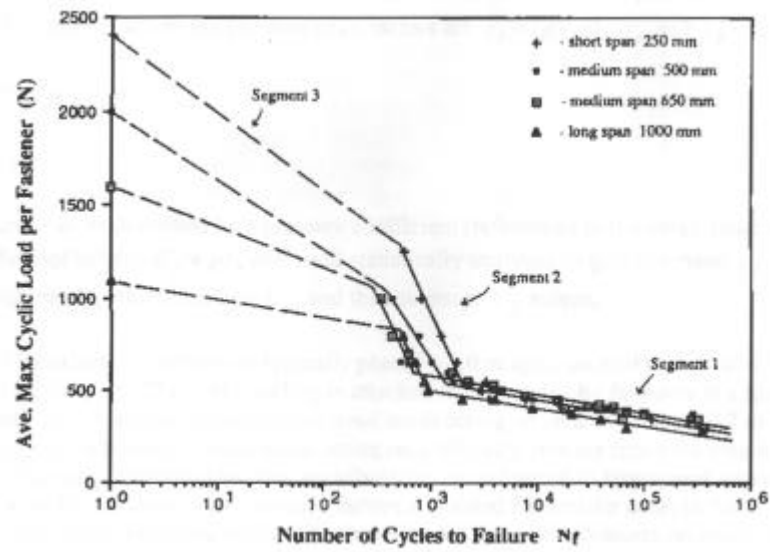


Figure 2.12 S-N curve for corrugated cladding fastened without cyclone washers [15]

Chapter 3 Experimental Method

A number of laboratory experiments were designed to investigate the fatigue behaviour of light gauge metal roof battens. The selected battens were subjected to a range of static and cyclic loads to obtain the static failure load and the fatigue performance. The Stramit Cyclonic Roof batten and the BHP Topspan 40 batten shown in Figures 3.1 and 3.2 were chosen for testing, as these are considered to be most commonly used in industry. The specification for the BHP and Stramit battens are given in Appendix A. The tests were formulated to establish the static capacity of the batten-truss connection, and results from the static tests were used to define the cyclic load bounds. Cyclic loads were applied at percentages of the average static capacity until failure. A range of cyclic tests were conducted at different percentages allowing an S-N curve to be developed. After obtaining the S-N curve, a series of block load tests were conducted to determine if Miner's rule could be used to predict the fatigue life of each batten.

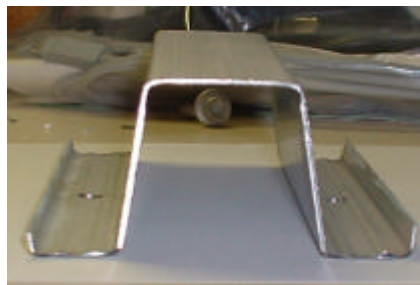


Figure 3.1 Cross-section of Stramit Cyclonic Roof batten



Figure 3.2 Cross-section of BHP Topspan 40 batten

3.1 Test Configuration

Tests were conducted on the INSTRON (model 1342) universal testing machine with a capacity of 100kN, in the structures lab at the School of Engineering, James Cook University. The INSTRON was calibrated using a proving ring before testing was undertaken. The calibration results are shown in Appendix B. A testing apparatus which simulated the batten-truss connection had to be designed in order to carry out the tests. The lengths of the test specimens were specified as 150 mm, allowing the testing apparatus to be designed to easily fit into the INSTRON. The apparatus was designed to allow the batten to be subjected to static and cyclic loads. This was done by ensuring the apparatus could apply a constant loading rate as well as a sinusoidal load to the batten. Figure 3.3 shows the batten-truss connection apparatus attached to the INSTRON and Figure 3.4 shows a schematic diagram of the testing apparatus. A SHS bar supports the top of the batten and is attached to the fixed ram on the INSTRON. The batten was bolted to the truss which was connected to the loading ram. Loads were applied by displacing the loading ram downwards at a constant rate for the static tests and by applying sinusoidal loading wave for the cyclic tests. However, the apparatus design was limited to bounds cycling from zero or greater to a nominated upper bound, simulating a suction loading.

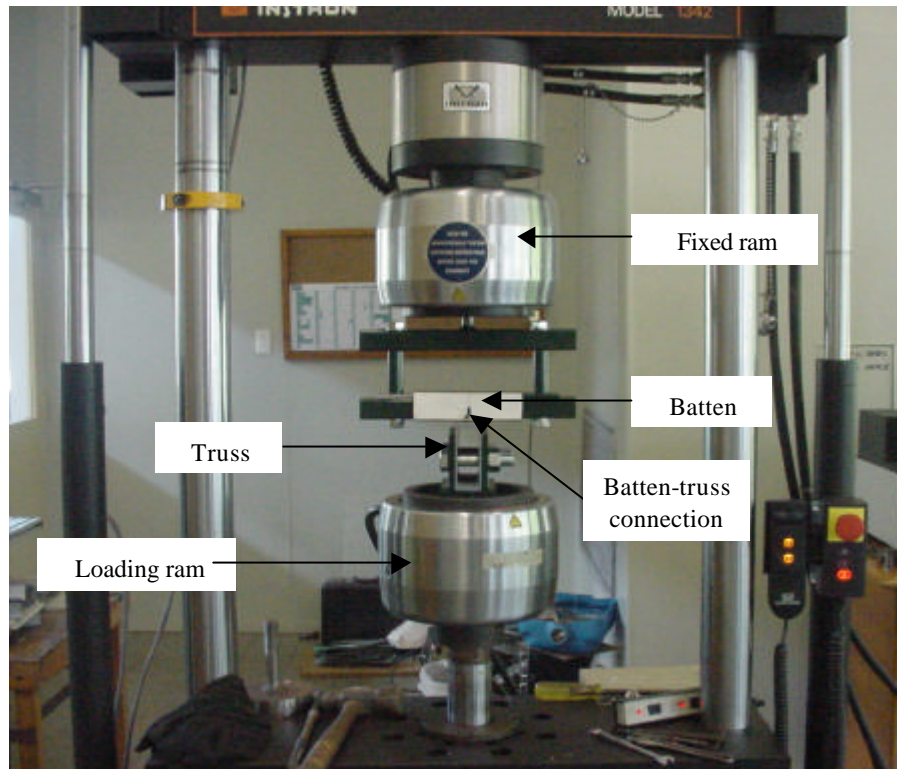


Figure 3.3 Test Setup

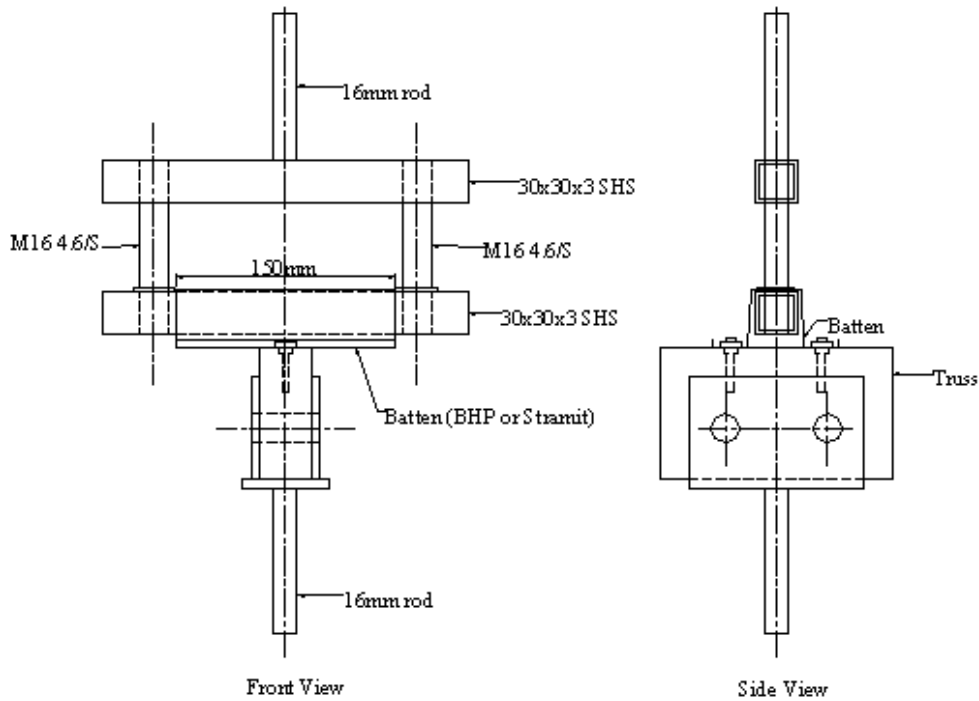


Figure 3.4 Schematic of testing apparatus (not to scale)

A number of trials were conducted to devise a satisfactory test setup. Initially the batten was attached to a timber truss however, the timber trusses encountered problems with splitting or screw failure. To overcome this problem a metal block was constructed from 6mm plate; two holes were predrilled in the top of the block so that the batten could be bolted to the truss. Washers were made up to the dimensions of the 12 gauge screw washer. The thickness of the washers were altered after the first two static tests as the thin washer was buckling and not simulating the screw washer. It was determined that a thicker washer with rounded edges (as sharp edges acted as a cutting tool), simulated the screw washer as shown in Figure 3.5. Figure 3.5 shows the comparison of the screw head used to fasten the battens to the timber trusses and the washer used in the laboratory experiments.



Figure 3.5 Batten screw (12 gauge) and washer used in laboratory experiments

3.2 Tensile Tests

A number of tensile tests were conducted on the batten material in the longitudinal direction. Test specimen dimensions were determined in accordance with AS1391 – methods for tensile testing of metals [4] and the selected test section dimensions are shown in Figure 3.6. The tests were carried out to determine the tensile strength of the batten material and to compare the experimental tensile strength with the specified minimum tensile strength of 550MPa. The width, thickness and initial length were measured using vernier callipers and used in calculating the tensile strength. The test specimens were loaded at 1mm/min and the INSTRON recorded the load, displacement and the maximum load reached. The tensile strength was calculated as follows:

$$R_m = \frac{F_m}{S_o} \quad (3.1)$$

where R_m is the tensile strength, F_m is the maximum force and S_o is the original cross-sectional area of the test piece within the gauge length.

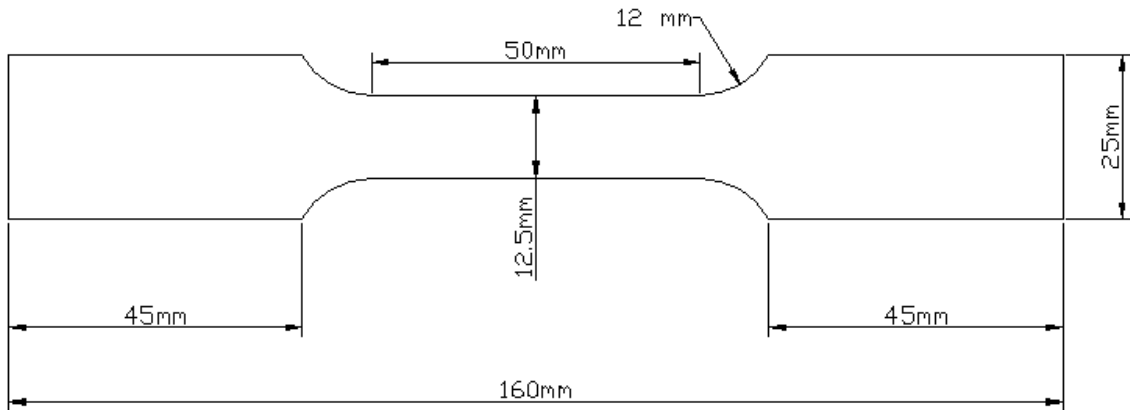


Figure 3.6 Tensile test dimensions (not to scale)

3.3 Static Tests

A series of static load tests were carried out on the BHP and Stramit battens, the failure load recorded, and the average failure loads were calculated for each batten type. Static tests were conducted by loading the INSTRON at a constant displacement rate until the batten disengaged from the truss connection. A 5mm/min loading rate was chosen for the static test with the INSTRON recording the load and displacement which was plotted and the failure load obtained.

3.4 Constant Amplitude Cyclic Tests

Determination of the average static failure load for the Stramit and BHP battens allows the upper loading bounds for the constant amplitude cyclic tests to be specified. The INSTRON was programmed to the required wave function, cycling frequency and cycling range. The sinusoidal wave function was used for the cyclic tests, which allows the INSTRON to cycle between an upper and lower load bound. Constant amplitude cyclic tests were conducted between bounds of zero to a percentage of the average static failure load. Cyclic loads were applied to the battens until disengagement from the connection and the number of cycles to failure were recorded and used to plot the S-N curve.

3.5 Block Cyclic Load Tests

The battens were subjected to blocks of loading cycles determined using the data obtained from the constant amplitude cyclic tests and the S-N curve. Assuming that Miner's Rule is applicable, pre-determined loading blocks were applied to the battens. The number of cycles and the percentage of the average static failure load the block cycled at were recorded. This was done for each loading block until the batten disengaged from the connection. Miner's rule was applied to the recorded results to determine if it is appropriate to predict the fatigue life of the batten. The loading sequence was also varied to determine if the order of loading had an effect on the fatigue performance, as it was noted in Chapter 2 that the order of loading is a critical factor for predicting roof cladding fatigue.

Chapter 4 Experimental Results, Discussion and Analysis

4.1 Tensile Tests

Tensile test were conducted on five test specimens taken from the BHP battens and five tests specimens taken from the Stramit battens. Tensile tests were conducted by applying a load at a constant rate, the failure load was recorded and given in Appendix C. The maximum load was used to calculate the tensile strength as shown in Table 4.1.

Table 4.1 Tensile test results

Sample No.	Tensile strength (MPa)
BHP 1	651.16
BHP 2	649.54
BHP 3	631.91
BHP 4	645.96
BHP 5	652.42
Average	646.20
Standard deviation	8.34
Coefficient of variation	1.29%
Sample No.	Tensile strength (MPa)
Stramit 1	651.60
Stramit 2	651.85
Stramit 3	654.08
Stramit 4	647.60
Stramit 5	643.14
Average	649.65
Standard deviation	4.32
Coefficient of variation	0.66%

The minimum specified tensile strength of the G550 batten material is 550MPa. Test results have determined that the tensile strength is approximately 650MPa verifying that the material specifications are satisfied. The BHP batten material was observed to have a greater variability in results than the Stramit batten. This variability in the results can be seen by comparing the coefficient of variation for each batten. The BHP batten coefficient of variation was calculated to be 1.29% as opposed to the Stramit coefficient of variation of 0.66%, these results deviate from each other by a factor of 2. However these tensile

tests were conducted on samples taken from one batten batch and to correctly determine if there is variability in the BHP batten material, additional tensile tests need to be carried out over a larger test range.

4.2 Static Tests

4.2.1 BHP Topspan 40 Batten

Static tests were performed on six BHP battens, with a number of static test trials conducted before the test setup was finalised. Detailed results for the trials and tests are given in Appendix D. A typical load vs. displacement curve from test results is shown in Figure 4.1. The load vs. displacement curve has two well defined peaks. An explanation for this is that both batten fasteners do not fail at the same time. The first peak is reached when the batten starts to fail on one side (crack initiation), and then the majority of the load is transferred to the other fastener until the batten tears around that fastener. Generally, the first peak load was higher; however for some tests the second peak was higher. In both cases the failure load was taken as the load at the first peak. Plots of load vs. displacement for the BHP battens are given in Appendix E. Summarised results for the six BHP static batten tests are shown in Table 4.2.

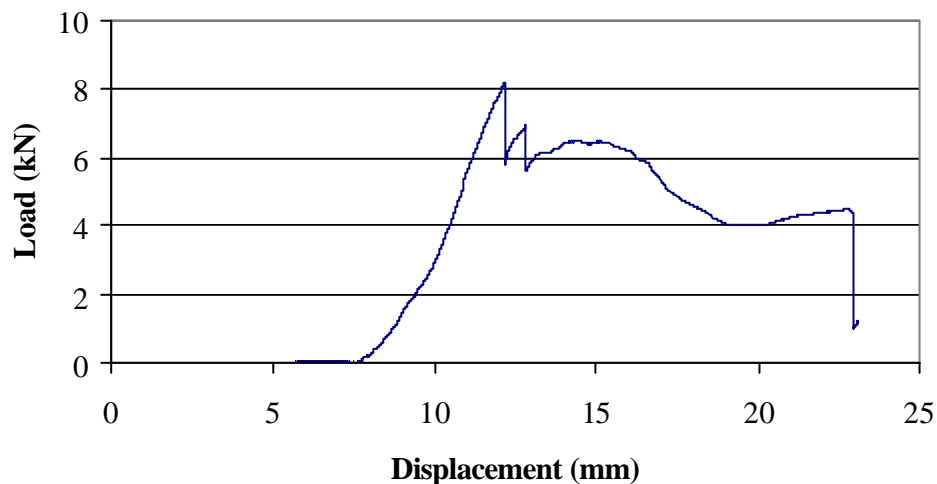


Figure 4.1 BHP Static Test load vs. displacement curve

Table 4.2 BHP Batten failure loads

Test No.	Failure Load (kN)
6	8.17
7	7.58
8	8.46
9	6.60
10	6.50
11	8.03
Average	7.56
Standard deviation	0.83
Coefficient of variation	11%

A typical static failure mode for the BHP batten consists of the crack pattern cutting out a semi-circular shape around the washer and angling out towards the edges of the batten, as seen in Figure 4.2. Another typical failure mode was the crack starting at the washer edge closest to the batten web and following along the web crease and then angling towards the edge, as seen in Figure 4.3. When comparing Figures 4.2 and 4.3 notice that the turned over edge in Figure 4.2 is narrower than the turned over edge in Figure 4.3. It was observed that disengagement of the batten from the connection occurred at this unsymmetric narrow turned over edge for all the BHP static load tests.



Figure 4.2 BHP batten static failure mode at narrow turned over edge



Figure 4.3 BHP batten static failure mode at the unsymmetric wider turned over edge

4.2.2 Stramit Cyclonic Roof Batten

Static load tests were performed on five Stramit roof batten samples. The INSTRON recorded the load and displacement, and the plot of the load vs. displacement enabled the failure load to be determined. Stramit battens behaved differently to the BHP battens, and two types of load vs. displacement curves were observed as shown in Figures 4.4 and 4.5. Type 1 load vs. displacement curve, Figure 4.4 has the two well defined peaks similar to the BHP battens and the explanation for this is the same for the BHP batten. Type 2 load vs. displacement curve (Figure 4.5) has only one well defined peak. The postulation for the behaviour of this curve is that the cracking occurred simultaneously at both the batten-truss connections. Summarised results from the five Stramit static tests were recorded and are shown in Table 4.3.

Observation of the tests results have shown that the BHP batten has a greater variation in results as opposed Stramit batten. The coefficient of variation is 11% and 6.37% for the BHP static tests and the Stramit static tests respectively. These coefficients of variation deviate approximately by a factor 2 similar to that observed with the tensile tests.

However the static test variation coefficients differ by a factor of 10 compared to the tensile test variation coefficient. The higher variability in the BHP batten results is ascribed to the variability in the material and the geometry of the batten

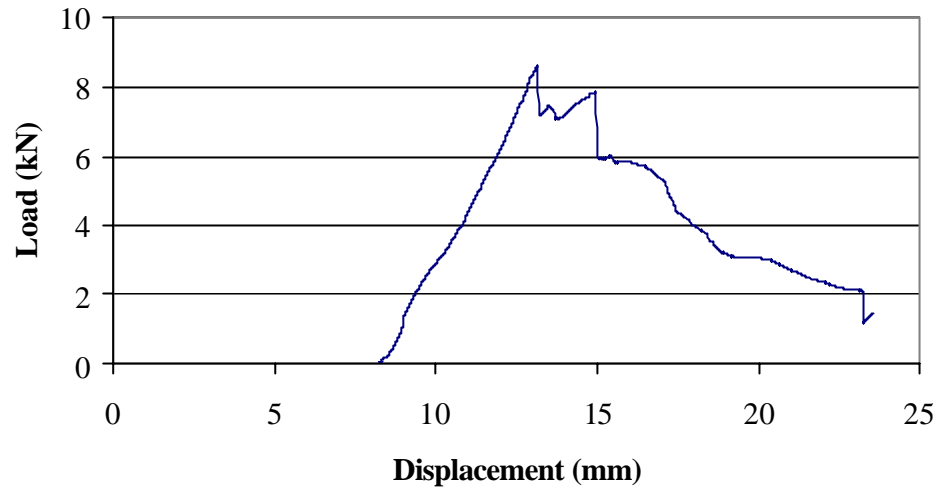


Figure 4.4 Type 1 Stramit static test load vs. displacement curve

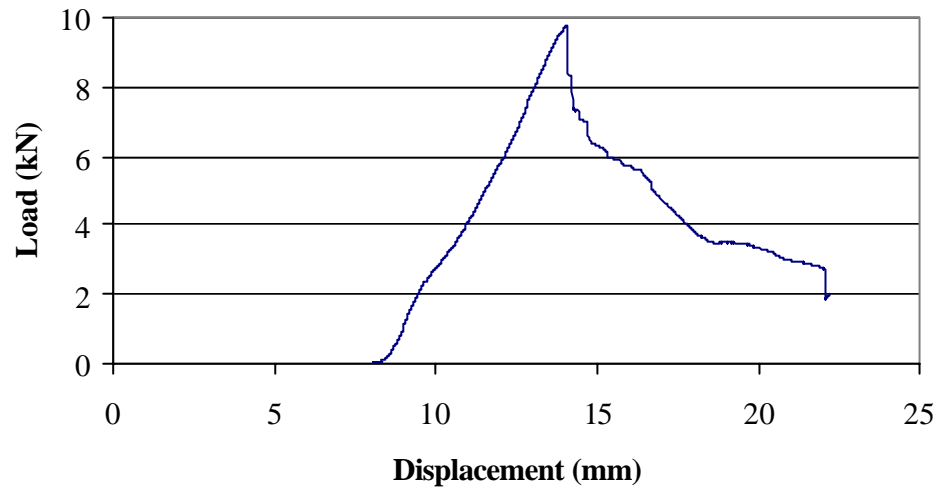


Figure 4.5 Type 2 Stramit static test load vs. displacement curve

Table 4.3 Stramit batten failure loads

Test No.	Failure Load (kN)
1	9.78
2	9.22
3	8.32
4	8.60
5	8.81
Average	8.95
Standard deviation	0.57
Coefficient of variation	6%

Typical observed failure modes for the Stramit batten are shown in Figures 4.6 and 4.7. Figure 4.6 shows the crack pattern following around the washer and moving longitudinally along the edge of the groove in the batten leg on one side and cracking to the edge on the other side. Figure 4.7 shows the batten cracking in a semi-circular pattern around the washer and then failing at the batten edge. Notice that the battens turned up edge is buckled next to the washer, where there are large stress concentrations.



Figure 4.6 Stramit Batten failure mode



Figure 4.7 Stramit Batten failure mode

4.3 Constant Amplitude Cyclic Tests

4.3.1 BHP Topspan 40 Batten

A series of constant amplitude cyclic tests were conducted at 80% of the average static failure load. However, a number of difficulties were encountered with the battens such as the washer tearing into the batten web on loading due to insufficient room caused by the wide turned over edge. The inability to tighten the bolt sufficiently due to the turned over leg edge was another difficulty encountered. As shown in Table 4.4 this caused varied results, with failure above 2000 cycles resulting from the bolt failing in fatigue. This was because the bolt was unable to be tightened sufficiently and the turned over edge causing unequal prying forces on the bolt. The very low cycles to failure were due to the washer cutting in to the batten web on initial loading of the batten, causing the batten to fail earlier than expected. These observations have shown the importance of simulating the batten hold down use in industry. Due to the restricted time limit of the project, further testing on the BHP batten was discontinued. Although these difficulties were encountered, it should be noted that the average static failure load is at least twice that of the battens specified design load. Therefore 80% of the average static failure load is well above the specified design load and the batten may behave differently at lower loads.

Table 4.4 Constant amplitude test results for BHP batten

Upper cycle bound (% of average static failure load)	Cyclic bound (kN)	No. of cycles till failure	Comments
80%	6.5	2830	Bolt failed due to fatigue
80%	6.5	195	Washer tore into web on loading, test continued until failure
80%	6.5	412	Washer tore into web on loading, test continued until failure
80%	6.5	2385	Bolt failed due to fatigue

4.3.2 Stramit Cyclonic Roof Batten

A number of constant amplitude cyclic tests were conducted, cycling between a lower bound of zero and an upper bound from between 40% to 80% of the average static failure load, with tests at 5% increments. A number of trial tests were conducted to determine the amplitude and frequency the INSTRON should be set at to achieve the best results for the required test bound. This was done to account for the force feedback controller of the INSTRON and the weight of the testing apparatus. Details of the INSTRON set up such as ramp, amplitude, frequency and detailed results are outlined in Appendix F. A load test was conducted at 30% of the average static failure load and took greater than 10,000 cycles to fail. Due to the time constraints of the research project, cyclic tests at loads lower than 40 % of the average static failure load were not considered. A summary of results for the constant amplitude cyclic tests are shown in Table 4.5.

Table 4.5 Constant amplitude test results for Stramit batten

Cycle bound (% of the static failure load)	Upper bound (kN)	No. of cycles till failure
85%	7.60	322
80%	7.20	394
75%	6.70	433
70%	6.30	677
65%	5.80	733
60%	5.40	1164
55%	4.90	1225
50%	4.50	1562
45%	4.00	2000
40%	3.60	3567

The results from the constant amplitude cyclic tests can be plotted to determine the S-N curve for the Stramit batten as described in Chapter 2. The load vs. number of cycles to failure (S-N curve) is well approximated by a straight line, shown in Figure 4.8. The equation for the line of best fit for the data points is found to be $S = 48.508N^{-3.22}$ where S is the stress amplitude in kN and N is the number of cycles to failure. The coefficient of determination (R^2) is 0.9755 giving a correlation coefficient $r = -\sqrt{0.9755}$. The negative

correlation coefficient indicates a negative slope and as one variable increases in this case the stress amplitude the other variable (the number of cycles to failure) decreases. This negative correlation coefficient of $r = -0.9877$ indicates that the S-N curve closely follows a linear relationship when $\log S$ is plotted against $\log N$. The closer the correlation coefficient is to 1 or -1 the stronger the linear relationship. To rearrange the formula into the form $NS^m = K$, which is used in determining fatigue damage under wide band random stress variations [13], $\log S$ must be plotted on the x axis and $\log N$ on the y axis as shown in Figure 4.9. This graph gives the equation $N = 150690S^{-3.0298}$ which can be rearranged to give $NS^{3.0298} = 150690$, where $m = 3.0298$ and $K = 150690$. This equation will be used later in finding the fatigue damage under wide band random stress variations.

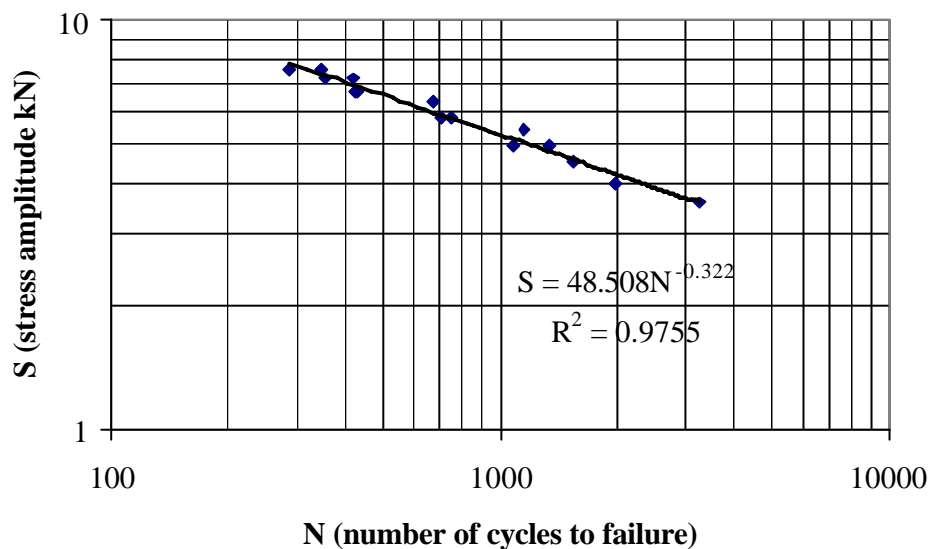


Figure 4.8 S-N curve for Stramit Cyclonic Roof batten

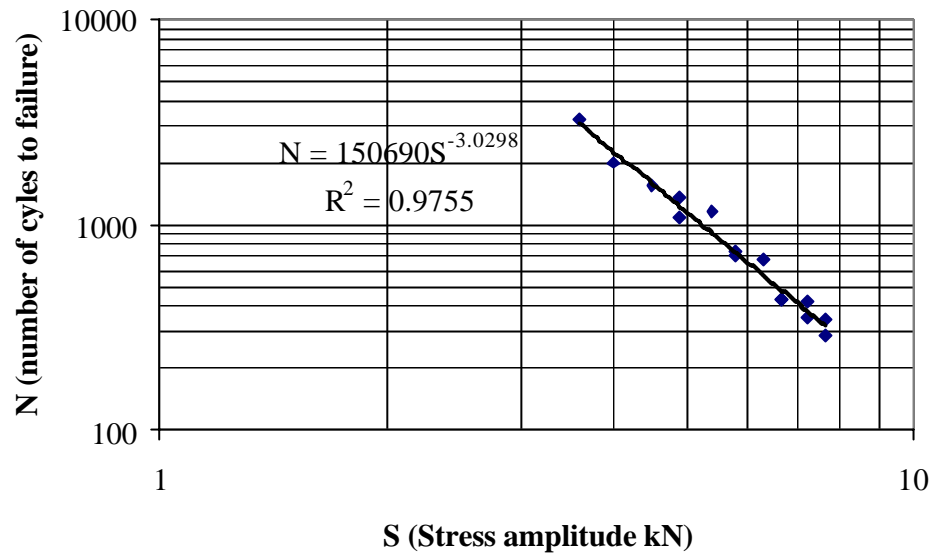


Figure 4.9 N-S curve for the Stramit batten

During the constant amplitude cyclic tests the batten's failure process was observed. The failure process consisted of the batten initially deforming plastically around the washer at the web crease and the turned up edge buckling in towards the washer where the stress concentrations were the highest. A 5 mm crack then formed on the underside of the batten, however at this stage it is not observed on the top side of the batten. The 5 mm crack then became visible on the top side of the batten and began to propagate longitudinally along the web crease. The crack progressed from a crack that opened and closed to a crack that stayed open due to the plastic deformation. Once the crack was open, disengagement of the batten from the truss connection was rapid, with the crack tearing out towards the edges in a failure mode shown in Figures 4.10, 4.11, 4.12, 4.13.

There are four noticeably different crack patterns for the constant amplitude cyclic tests as shown in Figures 4.10, 4.11, 4.12, and 4.13. Type A cracked longitudinally along the web crease and failed through the bolt hole, whereas Type B cracked longitudinally along the web crease and around the bolt hole, cutting a piece out. Type C and D cracked longitudinally along the web crease however, didn't fail along this crack instead failing at the bolt hole. Observations shown in Table 4.6 have found that crack Type A and B are

consistent with the higher loading greater than about 60% of the average static failure load, where as Type C and D crack pattern are associated with the load ranges lower than 60% of the average static failure load. Studies on cladding have found that this crack behaviour indicates a different fatigue response with the load levels giving a segmented S-N curve as shown in Figure 2.12. However, this does not look to be the case for the Stramit battens as the S-N curve can be well approximated by a straight line.



Figure 4.10 Type A

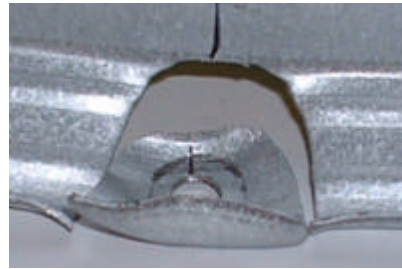


Figure 4.11 Type B

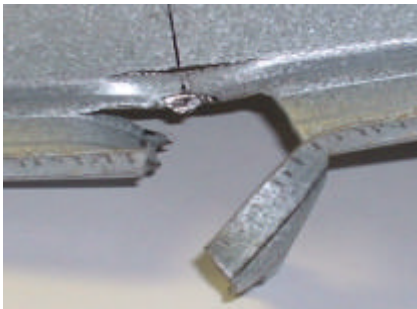


Figure 4.12 Type C



Figure 4.13 Type D

Table 4.6 Crack types at different load levels

Upper bound load (kN)	Upper bound % of average static failure load	Crack type at bolt hole 1	Crack type at bolt hole 2
7.6	85%	B	B
7.2	80%	B	A
6.7	75%	B	A
6.3	70%	A	A
5.8	65%	B	A
5.4	60%	A	B
4.9	55%	C	C
4.5	50%	D	C
4.0	45%	D	D
3.6	40%	C	C

Full scale tests have been conducted on 0.75 bmt top hat roof battens for a building located in cyclonic area by the Cyclone Testing Station in the large pressure airbox at James Cook University [19]. Inspections of the crack patterns on the battens tested in the airbox have found that the crack behaviour closely resembled the crack patterns observed in these laboratory tests. Figures 4.14 and 4.15 show the typical crack patterns observed on the battens tested by the Cyclone Testing Station. Figure 4.14 shows a longitudinal crack along the web crease and the batten failing by tearing around the screw. This pattern is similar to the crack behaviour seen in Figure 4.13 (Type D). Figure 4.15 shows the crack forming longitudinally along the web crease and failing through the screw hole. This pattern is similar to the crack behaviour seen in Figures 4.10 (Type A). Figures 4.10 and 4.11 show that for loads greater than 60% of the average static failure load, failure occurs along the web crease. However, Figures 4.12 and 4.13 shows the cracks form along the web crease but fail at the bolt hole, which is characteristic of the lower loads.



Figure 4.14 Batten failure in Cyclone Testing Station air-box test



Figure 4.15 Batten failure in Cyclone Testing Station air-box test

4.4 Block Loads

4.4.1 Stramit Cyclonic Roof Batten

For the purpose of these tests two different load amplitudes 50% and 70% of the static failure load were chosen and four different load combinations were tested. These were in the following load sequences:

- 50% - 70%
- 70% - 50%
- 50% - 70% - 50%
- 70% - 50% - 70%

Results from the block load tests shown in Table 4.7 are used in determining if Miner's Rule can predict the fatigue behaviour of the Stramit batten. Tests carried out on cladding have shown that the low-high-low block loads have a different failure mechanism to the high-low-high block loads. Table 4.7 shows the damage coefficient at failure of the Stramit batten under the range of block loads indicated.

Table 4.7 Block load test results

1 st block	No. cycles in 1 st Block	2 nd block	No. cycles in 2 nd block	3 rd block	No. cycles in 3 rd block	Cycles to failure at 50%	Cycles to failure at 70%	$\sum \frac{n_i}{N_i}$ at failure
50%	780	70%	100	n/a	n/a	1637	576	0.65
70%	340	50%	1495	n/a	n/a	1637	576	1.50
50%	390	70%	340	50%	801	1637	576	1.32
70%	170	50%	780	70%	170	1637	576	1.07

Note: Percentages are of the average static failure load

According to Miner's rule the sum of the proportion of cycles at a given stress level to the total number of cycles is equal to 1.0, at failure. That is,

$$\sum \frac{n_i}{N_i} = 1$$

The proportion of damage resulting from a range of block cycle loads $\sum \frac{n_i}{N_i}$ is defined as the damage coefficient. For a damage coefficient < 1.0 Miner's rule implies that failure does not take place, however for a damage coefficient > 1.0 the number of cycles to failure is exceeded.

Determining if Miner's rule can be applied to predict the fatigue life of the battens is difficult as the Stramit batten has shown similarities and differences to the fatigue performance of cladding. It was found that Miner's rule could not be used to predict the fatigue performance of cladding as different modes of crack initiation and propagation were observed indicating a different fatigue response depending on the load level [11]. Miner's rule relies on constant material properties and does not cope well with changing

profile shape, strength and stiffness. Different modes of cracking at different load levels were observed for the Stramit batten as shown in Figures 4.10 to 4.13 and may indicate that Miner's rule may not be satisfied.

The S-N curve for cladding was found to be segmented as shown in Figure 2.12 and could not be approximated by a single straight line. The Stramit batten S-N curve closely followed a straight line when $\log S$ is plotted against $\log N$, in this form it is often accepted that Miner's rule can be applied to determine the fatigue performance.

Results in Table 4.7 show that the sequence of applied loads of varying magnitudes produce different damage coefficients. Observations of the batten results in Table 4.7 show that if a lower load block is applied after crack initiation from a large load block the batten has a longer fatigue life and the damage coefficient is greater than if the higher block load is applied after crack initiation from a low load block. When analysing the damage coefficients at failure for each of the block load tests the results range between 0.65 and 1.5, which is within -35% to 50% of 1. However there is some variability in the test results and only four tests were conducted in which these observations are based on. To better understand if Miner's rule could be used to determine the fatigue performance of the batten, additional block cyclic load tests need to be conducted. A limited number of block cyclic load test results have shown some variability as the damage coefficients deviate from 1 by -35% to +50%. Miner's rule may be applied as a preliminary estimation for determining the damage caused to the batten until more block cyclic tests are conducted.

The crack initiation and propagation was closely observed and recorded for two constant amplitude cyclic tests. These observations were recorded at 80% and 70% of the average static failure load and are given in Appendix G. Failure occurred rapidly once an open crack was formed and for the purpose of discussion the open crack stage is defined as critical damage. Table 4.8 shows the number of cycles where it is estimated that critical damage is observed and the corresponding damage coefficient. The average damage coefficient for critical damage is 0.94. Miner's Rule has been accepted as a preliminary

estimation to determine the damage caused to the batten, therefore at failure the proportion of the cycles at a given stress to the total number of cycles is equal to 1.0. The mean damage coefficient of 0.94 for the critical damage supports the initial assumption that the batten failure can be adopted as disengagement from the connection. However, as there is evidence of different crack propagation at different load levels, this assumption needs to be confirmed through further testing and observation for load levels less than 60%.

Table 4.8 Critical damage coefficient

% of average static failure load	Estimated number of cycles at critical damage (n_i)	Number of cycles to failure (N_i)	$\sum \frac{n_i}{N_i}$
80%	350	380	0.92
70%	550	570	0.96

4.5 Application of loading regimes

Accepting that Miner's rule can be used to predict the fatigue life of the batten, cyclic pressure distributions from standard testing regimes such as TR440, DABM and L-H-L were applied and the damage coefficient $\sum \frac{n_i}{N_i}$ assigned for each test. TR440 is shown in Table 4.9, L-H-L shown in Table 4.10 and the DABM shown in Table 4.11. Parameters in the table columns are: n_i is the number of cycles, S_i is the load cycled at in kN and N_i is the number of cycles to failure at the load S_i . The load cycled at (S_i) was a percentage of the ultimate design load of the batten and the load percentage depended on the testing regime specifications. With the assumption that Miner's rule can be used it can be seen that the TR440 testing regime is the least severe regime giving a damage coefficient of 0.3, followed closely by the L-H-L with a damage coefficient of 0.43. Under the more conservative DABM the batten seems to only just fail with a damage coefficient of 1.03.

Table 4.9 Batten behaviour under TR440

TR440

cycle block	n_i	S_i (kN)	N_i
1	8000	1.52	42377
2	2000	1.90	21553
3	200	2.47	9734
4	1	4.94	1192

Damage coefficient 0.30
No batten failure

Table 4.10 Batten behaviour under L-H-L

L-H-L

cycle block	n_i	S_i (kN)	N_i
1	4500	1.71	29659
2	600	2.28	12405
3	75	2.85	6310
4	9	3.42	3632
5	1	3.80	2639
6	9	3.42	3632
7	75	2.85	6310
8	600	2.28	12405
9	4500	1.71	29659

Damage Coefficient 0.43
No batten failure

Table 4.11 Batten behaviour under DABM

DABM

cycle block	n_i	S_i (kN)	N_i
1	10000	2.47	9734
2	1	4.56	1519

Damage Coefficient 1.03
Batten failed

4.6 Fatigue Behaviour under Wind Loading

The rainflow count method is a cycle-counting technique that enables the simplification of complex loading sequences in a form suitable for fatigue analysis of structures, such as fatigue life prediction and simulation testing. Pressure measurements obtained on the 13.7 (b) x 9.1 (d) x 4.0 (h) m full-scale Texas Tech building were simplified using the rainflow count method to determine the number of pressure cycles and their means and ranges [10]. Using a design of Area B on the Texas Tech building shown in Figure 4.16 the fluctuating

pressure cycles were counted over a 15 min period and the C_p 's presented in Table 4.12,

where $C_p = \frac{P}{0.5 \rho_{air} \bar{U}_h^2}$ giving $p = 0.5 C_p \rho_{air} \bar{U}_h^2$. The 15 min pressure signal is assumed

to be represented 16 times to simulate a 4 hr design wind event.

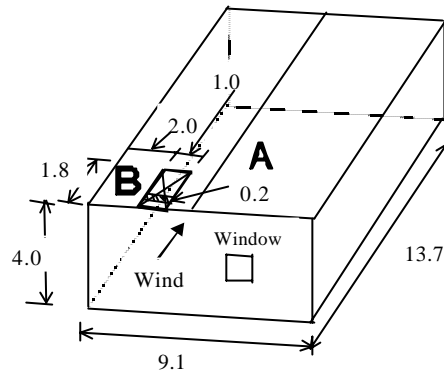


Figure 4.16 13.7 × 9.1 × 4.0 m full-scale Texas Tech building showing cladding-fastener tributary area A (1.0 × 0.2 m²) and batten-truss tributary area B (1.0 × 1.8 m²) [10]

Table 4.12 Area B Net Cps [10]

Range	5.72	5.09	4.45	3.82	3.18	2.54	1.91	1.27	0.64	0.00
	6.36	5.72	5.09	4.45	3.82	3.18	2.54	1.91	1.27	0.64
Mean										
0.0	0.64
-0.64	-1.27	120
-1.27	-1.91	9 1598
-1.91	-2.54	2	8	57	2680
-2.54	-3.18	.	.	.	1	2	5	10	26	67 1779
-3.18	-3.82	.	.	1	1	1	2	5	11	39 759
-3.82	-4.45	1	1	.	2	1	3	5	10	24 277
-4.45	-5.09	2	6	16	146
-5.09	-5.72	1	5	54
-5.72	-6.36	3
TOTAL		1	1	1	4	4	10	24	62	217 7416

Although laboratory tests involving different mean and range values have not been conducted on the batten truss, an analysis on the batten behaviour using the data from the Texas Tech building has been carried out. The means and ranges of the pressure fluctuation were considered to be a critical factor in the analysis of the fatigue behaviour of

cladding. However, due to time restrictions laboratory testing using different means and cycling bounds have not been conducted. To investigate the battens fatigue behaviour only the upper range will be analysed, and damage calculated using findings from the constant amplitude cyclic tests cycling between zero and an upper bound giving more conservative results. The pressure cycles are given in pressure coefficients (C_p) and therefore have to be converted into a pressure where p (kPa) is given by:

$$p = 0.5 \rho \bar{U}_h^2 C_p$$

where ρ is the density of air (1.2 kg/m^3) and \bar{U}_h is at 4m, \bar{U}_h is calculated by:

$$\frac{\bar{U}_{4m}}{\hat{U}_{10mTC2}} = 0.52 \quad [2]$$

where $\hat{U}_{10mTC2} = 70 \text{ m/s}$, the pressure is converted into a load (S) over an area of 1.2 m^2 for a typical domestic house roof system batten truss connection. Table 4.13 shows the pressure cycles and the fatigue behaviour. Results from this analysis show that the batten can undergo just over 8 hours of a sustained design wind events of similar nature to the pressure subjected to the Texas Tech building.

Table 4.13 Batten behaviour under pressure measurement from the Texas Tech building

U_{10mTC2} (m/s) =	70
U_{4m} (m/s) =	36.4
Tributary Area (m ²) =	1.2

Area B Net Cps

Upper Cp	p (kPa)	n _i	S _i (kN)	N _i
0.64	0.51	7416	0.61	671931
1.27	1.01	217	1.21	84253
1.91	1.52	62	1.82	24469
2.54	2.02	24	2.42	10316
3.18	2.53	10	3.03	5222
3.82	3.04	4	3.64	2996
4.45	3.54	4	4.25	1887
5.09	4.05	1	4.86	1256
5.72	4.55	1	5.46	882
6.36	5.06	1	6.07	639

Damage Coefficient	0.03	15 min duration
	0.44	4hr duration

Batten not failed

4.7 Narrow Band and Wide Band Damage

The fluctuating nature of wind loading produces fluctuating stresses in structures with contributions from resonant and background (sub-resonant) components. For most structures wide band background contribution is usually the dominant source of fatigue damage, however some wind loading situations produce resonant narrow-band vibrations. The fractional fatigue damage under wide band random stress variation can be written as:

$$D = ID_{nb} \quad [13]$$

where, D_{nb} is the damage calculated for narrow band vibration with the same standard deviation as the wide band vibrations. The value of I can be calculated by using the equation $I = a + (1 - a)(1 - e)^b$ given in Chapter 2 where e is found from the spectral density graph for the test data from the Texas tech building. From the spectral density graph $e = 0.84$ and the wide band damage $D = 0.44$, therefore the damage due to narrow band vibrations can be calculated. $D_{nb} = 0.52$ showing that more damage is caused by a narrow band vibration with the same standard deviation as the wide band vibration. Essentially the equation $D = ID_{nb}$ is used if the number of pressure cycles is counted

using the upcrossing method giving the narrow band damage. Wide band damage can be determined by calculating γ from the spectral density graph.

4.8 Cladding Fatigue vs. Batten Fatigue

A series of fatigue tests were carried out on Stramit battens using analysis methods for determining the fatigue behaviour of cladding. Both the batten and the cladding are manufactured from G550 coil, having a minimum yield stress of 550MPa. The mechanical properties vary in the longitudinal and the transverse direction of the coil. Studies have found that the cladding coil sheeting has a mean yield stress that exceeded 700MPa, with the mean yield stress in the longitudinal direction typically 720MPa and 780MPa in the transverse direction [11]. Due to the geometry of the battens only the longitudinal properties could be tested obtaining a tensile strength of approximately 650MPa and the yield strength of approximately 600MPa. The Stramit and BHP battens are 0.75mm bmt, and are specified for cyclonic areas, whereas the cladding is 0.42mm bmt. The process of cold working is used to obtain the desired bmt, this cold working process increases the yield strength of the material, hence the thinner the material the higher the yield stress. The fatigue behaviour of cladding is dependent on the load causing local plastic deformation (LPD), seen as dimpling under the screws around the fastener holes. The resistance to fatigue of the cladding increases noticeably if the cyclic load per fastener is kept well below the LPD load. Laboratory studies on the cladding have shown that a decreased block load following crack initiation from a higher block load, resulted in slower crack growth and longer life than if the higher load was continued. Whereas the opposite occurred if an increased block load followed crack initiation from a lower block load. Observations of the block cyclic load tests have also shown that this behaviour is a characteristic of the Stramit batten. However the damage coefficient at failure for the block cyclic load tests conducted only deviates from 1 by -35% and +50% and additional tests need to be conducted to account for the variability in the results.

Another similarity observed with the Stramit batten and the cladding is that different crack patterns occur at different load levels. Both the cladding and the batten have four different crack patterns shown in Figures 2.11 and 4.10 to 4.13. The four crack patterns for cladding

are associated with four different load levels. The load levels associated with the four different crack patterns are: loads well below the LPD load, loads approaching the LPD load, loads cycling through the LPD load and loads well above the LPD load. The Stramit battens crack behaviour however has two crack patterns associated with loads greater than 60% of the average static failure load, while the other two crack patterns are characteristic of loads less than 60% of the average static failure load. It was observed that for crack patterns of loads greater than 60% of the average static failure load, cracks initiated and propagated along the web crease and disengaged from the batten by cracking through the bolt hole or tearing around the washer (Figures 4.10 and 4.11). At loads lower than 60% of the average static failure load cracks formed longitudinally along the web crease however failed at the bolt hole. These different modes of crack initiation and propagation indicate a different fatigue response depending on the load level. The claddings different crack modes have been associated with a segmented S-N curve shown in Figure 2.12, however the S-N curve for the Stramit batten is closely approximated by a straight line.

Although the batten has shown characteristics of different fatigue response there are not enough results from the block cyclic load tests to clearly determine if Miner's rule can be used to determine the fatigue damage of the batten. Miner's rule has been accepted at this stage however, as there will be variability in the results. Additional block cyclic tests need to be conducted before concluding if Miner's rule can be used to predict the fatigue life of the batten.

Studies conducted on four different fastening assemblies for corrugated cladding have found that the fatigue behaviour is influenced by the way the cladding is fastened [20]. The four fastening assemblies investigated were cladding fastened without cyclone washers at alternate crests, cladding fastened with cyclone washers at alternate crests, cladding fastened without cyclone washer at every crest and the cladding fastened at alternate valleys. Each of the fastening assemblies performed differently and had differing S-N curves. Corrugated cladding fastened at alternate crests without cyclone washers showed a characteristic segmented S-N curve shown in Figure 2.12 previously discussed. Incorporating cyclone washers into the cladding assembly showed better fatigue

performance, smoothing out the S-N curve although it was still segmented. Cladding fastened without cyclone washers at every crest showed a characteristic S-N curve that was smooth and continuous, approximated closely by a straight line. Fastening the cladding at alternate valleys improved the fatigue performance markedly and smoothed the S-N curve out compared with the S-N curve for cladding fastened at alternate crests without cyclone washers [20]. From these observations it seems that the fatigue performance and the S-N curve may depend on the movement allowed by the fastener, the clearance between the mediums (i.e. the cladding and the batten and the batten leg and the truss) and the stress concentration area.

Cladding fastened without cyclone washers at alternate crests had the least restricted fastener assemble giving the worst fatigue properties out of the four assemblies. Studies conducted have shown that the fatigue behaviour can be improved with having tighter fasteners initially. These tighter screws decrease the clearance between the crest and the batten improving the fatigue properties. The tightened fasteners at the crest would create a reaction between the screw, the adjacent valleys and the batten spreading the fasteners load out over a greater area. Also the tightened fastener will increase the surface area the screw head sit on allowing stresses to be distributed over a larger area. However if the fastener is too tight, buckling is caused (LPD) which inturn results in premature fatigue failure. The tighter the fastener allows the cladding and the screw to act as one component whereas the looser screw and the cladding will act as separate entities, hence the cladding and the screw will act against each other in a jerking motion promoting quicker fatigue failure. The cladding fastened at every crest gives the most restricted movement in the fasteners, and has shown good fatigue properties and a smooth continuous S-N curve. Cladding fastened at alternate valleys gives minimal clearance between the cladding and the batten also showed good fatigue properties. Cladding fastened with cyclone washers distributes the stress concentration over a larger area and stiffens the screw restricting its movement improving the fatigue performance. However it did not behave as well as the cladding fastened at every crest and cladding fastened at alternate valleys. These two assemblies (cladding fastened at every crest and cladding fastened at alternate valleys) are not considered practical in the building industry. Cladding fastened at every crest causes

problems with timber splitting and cladding fasten at alternate valleys cause problems with water leaking and is primarily used on wall cladding. However from these fatigue performance observations it seems that the fatigue performance and the S-N curve may be governed by the fasteners tightness, the clearance between the mediums and the restriction of movement in the fastener. It is also considered that geometry affects the fatigue performance.

Observations from the cladding may be related to predict the performance of the batten. Results from the Stramit batten have shown that the S-N curve is well approximated by a straight line. From the observation previously outlined this is what would have been expected. The batten and the truss sit flush against each other and the fastener is able to sit flat on the batten leg, allowing limited movement in the fastener. Therefore the fastener can easily be tightened and will perform as one component with the batten. From these observations it would be expected that the BHP would have different fatigue behaviour due to its different geometry.

The presence of different crack patterns at different load levels would be expected. At loads close to the static failure load crack patterns would be similar to a static failure. Whereas at lower loads there is a longer time period for cracks to initiate, propagate and strain hardening to develop. This crack behaviour and the associated load levels have been discussed early in this chapter.

Chapter 5 Conclusions and Recommendations

The fatigue behaviour of top hat metal battens used in domestic house construction was investigated in this thesis. The BHP Topspan 40 and the Stramit Cyclonic Roof battens were chosen for testing as they were considered to be commonly used in industry. Tensile tests were conducted on the batten material in the longitudinal direction to verify the material specifications. A number of static test were carried out on each of the battens to determine the average static failure load. This average static failure load was used to obtain the upper bounds for constant amplitude cyclic tests. A series of constant amplitude tests were conducted cycling between zero and an upper bound. A number of difficulties were encountered with the BHP batten such as the washer tearing into the web on loading and difficulty with the bolt, being unable to tighten it sufficiently due to the turned over edges. These difficulties have demonstrated the need for correct replication of in practice hold down and the sensitivity of the battens performance to the hold down conditions. It was also observed with the BHP batten that the geometry was unsymmetrical, with one turned over edge being thicker and more flattened down than the other. Due to these difficulties with the BHP batten and the restricted time of the project, testing on the batten was discontinued.

An S-N curve was developed for the Stramit batten using the experimental results from the constant amplitude cyclic tests. The S-N curve was closely approximated by a straight line when $\log S$ was plotted against $\log N$. Block loading tests conducted on the Stramit batten verified that Miner's rule could be applied as a preliminary estimate to predict the fatigue life of the batten. Testing regimes were analysed theoretically to determine the batten fatigue behaviour under these tests. The batten's fatigue behaviour was analysed using methods applied to determine the fatigue characteristics of cladding. Results from this research can be used as a basis for an extended study in the fatigue behaviour of battens. The following conclusions and recommendations have been made based on the fatigue investigation.

5.1 Conclusions

- Tensile tests conducted on specimens taken from the longitudinal section of the batten material found that the tensile strength was approximately 650MPa.
- Static test results have shown that the BHP batten has an average static failure load of 7.56kN and the Stramit batten has an average static failure load of 8.95kN. The variability in the BHP static test results can be attributed partly to the batten's geometry and difficulties with the turned over edges and the washer tearing into the web on initial loading.
- Correct replication of the BHP battens hold down used in industry is necessary as this affects the batten fatigue behaviour. This caused difficulties with the BHP batten such as the washer tearing into the web and the bolt failing in fatigue instead of the batten. The turned over edge on the BHP batten causes the washer to sit on an angle and dig into the web where as if the bolt isn't tightened sufficiently the bolt fails instead of the batten.
- The S-N curve for the Stramit batten is closely approximated by a single straight line as opposed to the segmented S-N curve obtained for cladding.
- The Stramit batten has shown crack patterns that are characteristic of different load levels similar to the cladding. Four crack patterns were observed, with two crack patterns associated with loads greater than 60% of the average static failure load and the other two correlated with loads less than 60% of the average static failure load.
- It is shown that Miner's rule can be used as a preliminary means of predicting the fatigue life of the Stramit batten. There is some variability in the results and additional block cyclic load tests need to be conducted to make an adequate conclusion on the applicability of Miner's rule to predict the battens fatigue damage.
- The BHP and Stramit battens average static failure load is approximately twice the ultimate design load for the specified batten layouts.
- The Stramit batten has a damage coefficient of 0.3 and 0.43 for the TR440 and L-H-L testing regime respectively. A 4 hour design wind event was also theoretically analysed for the batten giving a damage coefficient of 0.44. These results show that the Stramit batten is likely to withstand an 8 hour design wind event. It can also be

seen that the L-H-L testing regime is a better representation of a 4 hour design wind event.

- Batten failure can be defined as disengagement of the batten from the connection. Miner's rule has been accepted as a preliminary estimation for damage caused to the batten and the mean critical damage coefficient is 0.94, hence being close to 1.0 which is the failure criterion for Miner's rule.
- The fatigue behaviour of the battens is found to be dependent on the fastener tightness, the clearance between the mediums (i.e. batten leg and the truss), the area of stress concentration and the batten geometry.

5.2 Recommendations

- In order to determine if Miner's rule can be accepted to correctly determine the fatigue life of the Stramit batten, additional block load combinations should be applied at different load levels.
- Studies of other 0.75 bmt battens should be conducted to determine if different geometries will have an impact on the failure mechanism similar to the cladding fatigue behaviour.
- Testing on the battens should be conducted by replicating the correct batten hold down used in industry as it has been observed from the BHP batten that the fatigue performance is sensitive to the hold down conditions.
- A number of cyclic tests should be conducted at a range of mean load levels representative of wind load characteristics. This will enable a better understanding of the fatigue behaviour at different means and load ranges.
- Fatigue tests were only conducted on the batten connection and the affect of torsion and bending was not taken into consideration. Once sufficient information has been gathered on the fatigue performance on the batten-truss connection testing procedures should be devised to investigate affects of torsion and bending.
- The Stramit batten has exhibited good fatigue performance and investigations into the batten fastener should be conducted to determine if the fastener will fail in fatigue before the batten.

- Studies of the thinner gauge steel battens should be conducted to determine if the different metal thicknesses will have an impact on the fatigue response.

References

1. Amzallag, C., Gerey, J. P., Robert, J. L and Bahuaud, J., (1994) “Standardization of the Rainflow Counting Method for Fatigue Analysis”, *Fatigue* Vol 16, 287-293.
2. AS1170.2 (1989). “Structural design actions Part 2: Wind actions”. Standards Association of Australia.
3. AS1170.2 (2002). “Structural design actions Part 2: Wind actions”. Standards Association of Australia.
4. AS1391 (1991). “Methods for tensile testing of metals”. Standards Association of Australia.
5. AS4040.3 (1992). “Methods of testing sheet roof and wall cladding – Resistance to wind pressure for cyclone regions”. Standards Association of Australia.
6. AS4055 (1992). “Wind loads for housing”. Standards Association of Australia.
7. Building Code of Australia. (1990). “Northern Territory Appendix”.
8. Dowling, N.E. (1999). “Mechanical Behavior of Materials – Engineering Methods for Deformation, Fracture, and Fatigue”. Prentice-Hall, New Jersey.
9. Ginger, J.D. (2001). “Characteristics of wind loads on roof cladding and fixings”. *Wind and Structures An International Journal*, Vol. 4, No. 1, 73 – 84.
10. Ginger J and Henderson D (2003). “Wind Loads on Roof Cladding and Fixings”. Cyclone Testing Station, School of Engineering, James Cook University, Townsville.
11. Henderson, D, Ginger, J and Reardon, G, (2001) “Performance of light gauge metal roof cladding subjected to cyclonic wind loading – A review” Cyclone Structural Testing Station, School of Engineering, James Cook University.
12. Holmes, J.D, (2001). “Wind Loading of Structures”. Spon Press, London.
13. Holmes, J.D. (2002). “Fatigue life under along-wind loading – closed-form solutions”. *Engineering Structures* 24, 109-114.
14. Kasper, D, (2002). “Fatigue failure of roof sheeting subjected to wind loading”. Thesis - James Cook University, School of Engineering.
15. Mahendran, M. (1989). “Fatigue behaviour of corrugated roofing under cyclic wind loading”. James Cook CSTS Technical Report No. 35.

16. Mahendran, M. (1993). "Simulation of cyclonic wind forces on roof claddings by random block load testing". James Cook CSTS Technical Report No. 38.
17. Mahendran, M. (1993). "Towards an appropriate fatigue loading sequence for roof cladding in cyclone prone areas". Physical Infrastructure Centre, Research report 93-20, QUT
18. Mahendran, M (2001). "Design of Steel Roof and Wall Cladding Systems for Pull-Out Failures". Steel Construction, Vol. 35, No.1.
19. Private communication with the Cyclone Testing Station, School of Engineering, James Cook University.
20. Robertson, A.P, Holmes, J.D and Smith, B.W (2003). "Calibrations of Closed-Formed Solutions of Fatigue Life Under Along-Wind Loading" 10AWES Workshop, Sydney
21. Smith, R. N. L., (1991) "Basic Fracture Mechanics", Butterworth-Heinemann Ltd, Oxford.
22. TR440 (1983). "Guidelines for the testing and evaluation of products for cyclone-prone areas". Experimental building station Department of housing and construction.
23. Xu, Y.L. (1993). "Wind-induced fatigue loading on roof cladding of low-rise buildings". James Cook CSTS Technical Report No. 41.
24. Xu, Y.L, Reardon, G.F. (1992). "Behaviour of different profiled roofing sheets subjected to wind uplift". James Cook CSTS Technical Report No. 37.

Appendix A

Batten Specifications and Design Capacity Tables

Stramit Cyclonic Roof Batten Specifications

(Taken from Stramit Top Hats & Battens Capacity Tables product technical manual)

SELECTION & SPECIFICATION**Features**

- High tensile steel – for high strength and low weight
- Quality products – with Stramit's proven record for manufacture and supply
- Limit-state design data – for fully conforming designs
- Fully tested – for technical confidence
- Rolled safety edges on roof and ceiling battens – to enhance user confidence
- Knurled anti-slip surfaces on roof and ceiling battens – for easier fastening

Applications

The range of **Stramit® Top Hats** is ideal for small to medium sized sheds and similar structures. **Stramit® Roof Battens** have been developed specifically for domestic applications but may be used in small commercial structures as well, with **Stramit® Cyclonic Roof Battens** having enhanced performance to endure the repeated loadings that can be experienced in tropical cyclones. **Stramit® Ceiling Battens** are intended for use with plasterboard sheeting in both domestic and commercial situations.

Materials

Stramit® Top Hats & Battens are manufactured from high-tensile (G550/G500) steel with either AZ150 zinc-aluminium alloy or Z350 galvanised coating in full conformance with AS1397.

Specification

Maintaining the structural integrity of a building structure is important. Even an apparently small change in product material or dimensions can lead to a considerable reduction in performance. One of the best ways to ensure structural adequacy is to prepare and enforce an appropriate specification for structural components.

A suggested specification is:

"All top hats/roof battens/ceiling battens shall be Stramit sections or approved equivalent supported by submission of section properties and capacity calculations/data in accordance with AS4600, AS3623 and AS1562. All sections shall be produced from high-tensile G500/G550 steel with a galvanised/zinc-aluminium alloy coating conforming to AS1397. All sections must be installed in accordance with the manufacturers recommendations with particular reference to the number, size, grade and positioning of fasteners."

Adverse Conditions

Stramit® Top Hats and Battens will give excellent durability in most applications. In exposed conditions, unwashed areas subject to salt-laden air or other corrosive matter may need additional protection. **Stramit® Top Hats and Battens** are not recommended for use in enclosed areas within 450mm of moist soil.

Compatibility

Contact between galvanised steel and copper (e.g. pipework) must be avoided as premature corrosion will occur.

STRAMIT® TOP HATS & BATTENS – PRODUCT THICKNESS, GRADE AND MASS

product	thickness bmt	steel grade	mass
Stramit® Top Hat TH64075	0.75 mm	G550	1.26 kg/m
Stramit® Top Hat TH64100	1.00 mm	G550	1.67 kg/m
Stramit® Top Hat TH64120	1.20 mm	G500	2.00 kg/m
Stramit® Top Hat TH96075	0.75 mm	G550	1.65 kg/m
Stramit® Top Hat TH96100	1.00 mm	G550	2.18 kg/m
Stramit® Top Hat TH96120	1.20 mm	G500	2.60 kg/m
Stramit® Roof Batten	0.55 mm	G550	0.77 kg/m
Stramit® Cyclonic Roof Batten	0.75 mm	G550	0.98 kg/m
Stramit® Ceiling Batten	0.42 mm	G550	0.37 kg/m
Stramit® Perth Ceiling Batten	0.42 mm	G550	0.34 kg/m

DESIGN DATA

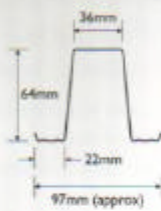
General

Stramit recommends that all designs conform to relevant Australian Standards such as AS1170 series (Loading Codes), AS4600 (Cold-formed steel structures) and AS3623 (Domestic metal framing).

Sizes

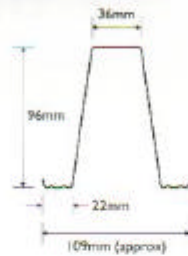
Stramit® Top Hat

TH64 series



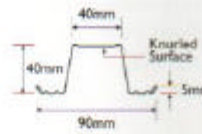
Stramit® Top Hat
TH64075, TH64100, TH64120

TH96 series

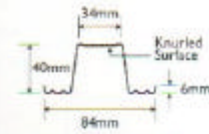


Stramit® Top Hat
TH96075, TH96100, TH96120

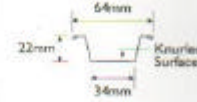
Stramit® Battens



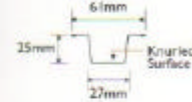
Stramit®
Roof Batten



Stramit® Cyclonic
Roof Batten



Stramit®
Ceiling Batten



Stramit® Perth
Ceiling Batten

Section Properties

STRAMIT® TOP HATS & BATTENS – FULL SECTION PROPERTIES

Section	Area A_g mm ²	I_x 10 ⁶ mm ⁴	I_y 10 ⁶ mm ⁴	Z_x^+ 10 ³ mm ³	Z_x^- 10 ³ mm ³	Z_y^+ 10 ³ mm ³	Z_y^- 10 ³ mm ³	r_x mm	r_y mm	I mm ⁴	β_x mm	I_w 10 ⁶ mm ⁴
Stramit® Top Hat TH64075	157	90.4	83.7	2.62	3.06	1.97	1.97	24.0	23.1	29.4	109	25.0
Stramit® Top Hat TH64100	208	120	111	3.48	4.03	2.61	2.61	24.0	23.1	69.4	109	32.5
Stramit® Top Hat TH64120	253	147	166	4.22	4.93	3.51	3.51	24.1	25.6	122	110	41.1
Stramit® Top Hat TH96075	206	245	152	4.80	5.44	2.99	2.99	34.5	27.1	38.7	157	63.8
Stramit® Top Hat TH96100	274	325	202	6.39	7.17	3.98	3.98	34.4	27.1	91.4	158	82.8
Stramit® Top Hat TH96120	328	389	242	7.65	8.53	4.77	4.77	34.4	27.1	158	158	97.3
Stramit® Roof Batten	92.1	23.7	67.8	1.13	1.25	1.37	1.37	16.0	27.1	9.28	87.8	7.56
Stramit® Cyclonic Roof Batten	120	29.5	68.9	1.36	1.62	1.62	1.62	15.7	24.0	22.5	78.0	8.84
Stramit® Ceiling Batten	43.2	3.56	16.0	0.34	0.31	0.47	0.47	9.09	18.3	2.54	62.6	0.45
Stramit® Perth Ceiling Batten	43.4	4.43	13.3	0.37	0.34	0.43	0.43	10.1	17.5	2.55	60.0	0.50

STRAMIT® TOP HATS & BATTENS – EFFECTIVE SECTION PROPERTIES

Section	Area A_e/f_y mm ²	I_{e_x} 10 ⁶ mm ⁴	I_{e_y} 10 ⁶ mm ⁴	I_{e_x} 10 ⁶ mm ⁴	I_{e_y} 10 ⁶ mm ⁴	Z_x^+ 10 ³ mm ³	Z_x^- 10 ³ mm ³	Z_y^+ 10 ³ mm ³	Z_y^- 10 ³ mm ³
Stramit® Top Hat TH64075	91.0	87.0	82.6	74.0	74.0	2.59	2.30	1.62	1.62
Stramit® Top Hat TH64100	141	116	116	102	102	3.44	3.29	2.29	2.29
Stramit® Top Hat TH64120	188	143	145	156	156	4.18	4.16	3.20	3.20
Stramit® Top Hat TH96075	92.0	236	200	118	118	4.73	3.49	2.05	2.05
Stramit® Top Hat TH96100	144	315	315	165	165	6.30	6.10	2.93	2.93
Stramit® Top Hat TH96120	192	382	386	204	204	7.59	7.57	3.69	3.69
Stramit® Roof Batten	51.5	20.8	18.6	62.0	62.0	1.00	0.79	1.20	1.20
Stramit® Cyclonic Roof Batten	85.3	28.0	26.5	66.6	66.6	1.34	1.16	1.53	1.53
Stramit® Ceiling Batten	26.7	2.86	2.72	15.6	15.6	0.22	0.22	0.45	0.45
Stramit® Perth Ceiling Batten	26.2	3.55	3.54	12.6	12.6	0.24	0.25	0.39	0.39

Stramit® Roof Battens

Stramit® Roof Battens may be used with either metal sheeting or with concrete/terracotta tiles. The relevant performance can be obtained from the following sections.

TILES

Based on the foot traffic requirements of AS3623 the maximum span for Stramit® 0.55 Roof Batten is 1200mm. This assumes a maximum batten spacing of 300mm and a maximum tile weight of 0.67 kPa.

METAL ROOFING

DARWIN DEEMED-TO-COMPLY

The Northern Territory Building Advisory Committee has approved the Stramit® Cyclonic Roof Batten for use in the Darwin area. Each application must conform to the specific details outlined in Design Data Sheets M/630/1 and M/630/2. These sheets are contained within the Darwin Cyclone Area Building Manual or can be obtained from the local Stramit office.

STRAMIT® 0.55 ROOF BATTENS MAXIMUM BATTEN SPACINGS (mm) #																				
AS4055 Load Category Wind Pressure (kPa) #	Truss spacing (mm), fastening and truss material								Stramit® sheeting, thickness bmt (mm) & fastening per sheet per batten											
	2 x No12 screws into 1.5 G450, 2 x No10 screws into 1.9 G450, or 2 x No10 type 17s lisa timber				2 x No10 screws into 1.0 G550				Monoclad®		Corrugated		Longspan®		Speed Deck Ultra®					
	450	600	900	1200	450	600	900	1200	0.42	0.48	0.42	0.48	0.42	0.48	0.42	0.48				
								4 screws	3 scr	5 scr	3 scr	5 scr	3 scr	5 scr	3 scr	5 scr	1 clip & 3 scr			
N1 1.35	2200	2200	2200	1750	2200	2200	1780	1330	1350	1700	900	900	1200	1200	1750	1750	2250	2250	1700	2300
N2 1.94	2200	2200	2140	1250	2200	1900	1270	950	1350	1700	900	900	1200	1200	1750	1750	2250	2250	1700	2300
N3 2.96	2200	2060	1370	800	1670	1220	810	610	1350	1700	900	900	1200	1200	1550	1750	1550	2100	1550	1550
N4 4.43	1830	1380	920	530	1090	810	540	400	1250	1250	900	900	950	1200	-	1400	1050	1400	1050	1050
N5 6.53	1270	950	630	370	750	560	370	-	850	850	-	900	650	1100	-	950	-	950	700	700
N6 8.84	930	700	460	-	550	410	-	-	-	-	-	800	450	800	-	-	-	700	-	-

STRAMIT® 0.75 CYCLONIC ROOF BATTENS MAXIMUM BATTEN SPACINGS (mm) #																		
AS4053 Load Category Wind Pressure (kPa) #	Truss spacing (mm), fastening and truss material								Stramit® sheeting, thickness bmt (mm) & fastening per sheet per batten									
	1 x No12 screws into 1.5 G450, 1 x No10 screws into 1.9 G450, or 2 x No10 type 17s lisa timber				2 x No10 screws into 1.0 G550				Monoclad®		Corrugated		Longspan®		Paneldek® 200 400		Speed Deck Ultra®	
	450	600	900	1200	450	600	900	1200	0.42	0.48	0.42	0.48	0.42	0.48	0.55	0.55	0.42	0.48
								4 assy	5 assy	5 assy	4 assy	4 assy	clip & screws	clip & screws	clip & screws	clip & screws	1 clip & 3 screws	1 clip & 3 screws
C1 3.71	2200	1710	1140	850	1300	970	650	480	1200	1200	900	1100	1300	1300	1100	1000	1000	1000
C2 5.54	1520	1140	760	570	870	650	430	320	800	800	800	1000	800	850	750	750	650	650
C3 8.17	1050	780	520	390	600	450	300	-	550	550	550	650	600	600	500	500	450	450
C4 11.05	770	580	380	-	440	330	-	-	400	400	-	500	400	400	350	-	-	-

Note that at the truss spacings (batten spans) shown foot traffic loads to AS1562 have been accounted for.

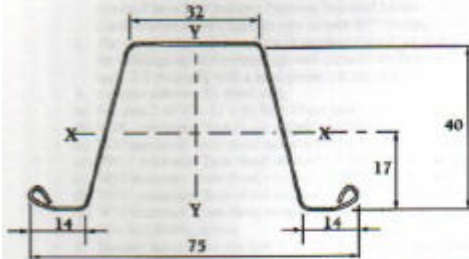
Strength limit-state wind pressures in accordance with AS4055, allowing for local pressure areas.

The apparent anomaly that at higher pressures some profile spans are longer than for higher performing products is due to the limitation being solely related to the number of fastenings into the batten. Products with more closely spaced fasteners will have an increased capacity in these circumstances.

- Spans may be limited by sheeting selection – see right-hand columns.
- Spans will be limited by sheeting selection – see right-hand columns.
- Spans may be limited by truss selection – see left-hand columns.
- Spans will be limited by truss selection – see left-hand columns.

BHP Topspan 40 Batten Specification
 (Taken from BHP Topspan Steel Roof Battens BHP building products brochure)

**Economical Steel Roof Battens
 for Non-Cyclonic Areas**



TOPSPAN® 40 roof battens from BHP Building Products are the economical alternative to timber roof battens. Made from hi-tensile Australian steel, TOPSPAN 40 roof battens are lighter than timber battens and because they will nest together, storage, carrying and handling are made easier.

TOPSPAN 40 battens can be lapped, saving the time consuming process of cutting to length and so making them quicker and easier to install. Their consistent straightness simplifies alignment, and fastening is quick and easy using self-drilling screws.

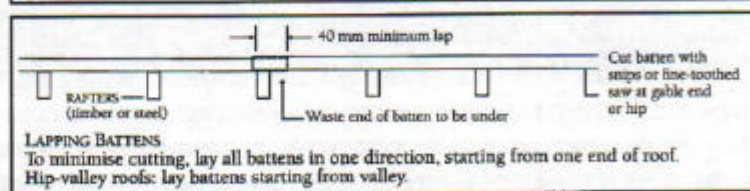
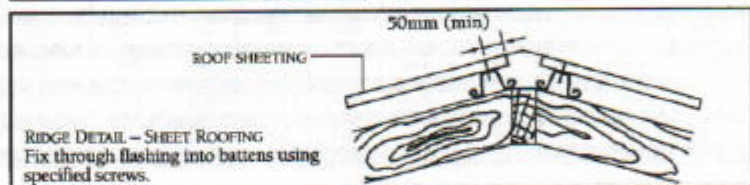
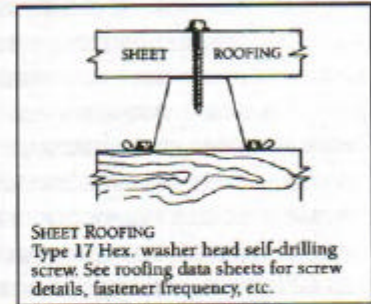
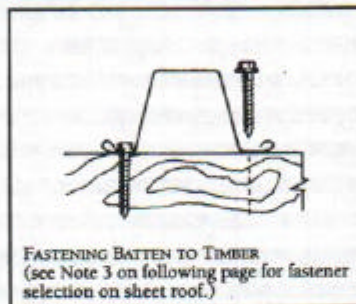
Batten ends are mitre-cut for simple installation at hip and valleys and the rolled edges on TOPSPAN 40 battens provide added safety when handling.

Material Specifications

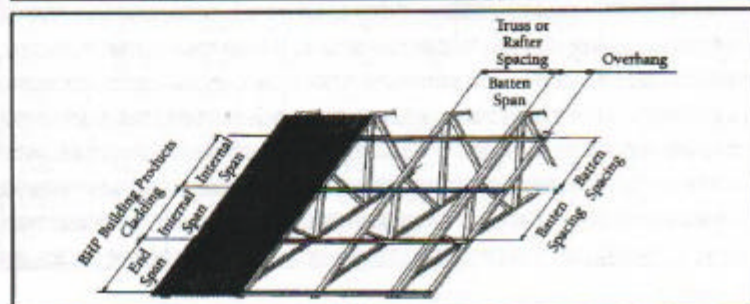
TOPSPAN 40 battens are manufactured from BHP ZINCALUME® steel complying with AS1397-G550-AZ150 (550 MPa minimum yield strength, 150 g/m² minimum coating mass).

Thickness (mm) (BMT)	0.55
Yield Strength (MPa)	550
Coating Mass (g/m ²)	150
Mass (kg/m)	0.62

Installation



Allowable Batten Spacing



Allowable Batten Spacing In Non-Cyclonic Areas

- Notes:
- The tables are based on a general design approach. The tables will give a practical and economic solution for most domestic buildings in non-cyclonic areas. For specific design situations, information on fastener and batten capacity may be obtained from BHP Building Products Technical Advisory Service (all relevant details should be forwarded to your nearest BHP Building Products office).
 - The design pressures have been determined from AS1170 Part 2, 1989, Section 3, for buildings up to 6 metres high with pressure coefficients of +0.2 internally and -0.9 externally with a local pressure factor of 1.5.
 - Fastener selection for sheet roof:
 - For pine 2 off 12 x 40 Type 17 per joint
 - W28 - minimum Truss chord material 1.0 BMT - 2 off 10 - 16 x 16*
 - W33 - minimum Truss chord material 1.0 BMT - 2 off 10 - 16 x 16*
 - W41 - minimum Truss chord material 1.0 BMT - 2 off 10 - 16 x 16*
 - W50 - minimum Truss chord material 1.2 BMT - 2 off 12 - 14 x 20*
 - W60 - minimum Truss chord material 1.2 BMT - 2 off 12 - 14 x 20*
 - W70 - minimum Truss chord material 1.6 BMT - 2 off 12 - 14 x 20*
 - Fastener selection for tile roof: 1 off 10 - 16 x 16 Hex. self drilling screws per

- joint alternating top and bottom. Use 2 per joint at free ends.
- Fastener selection for cladding: 12 gauge Type 17 or 12 - 11 reduced drill point as per standard BHP Building Products recommendations.
- The maximum batten span is 1200 mm for sheet or tile roof.
- Roof truss design may be based on a maximum batten spacing. The designer/fabricator should be contacted for this information. BHP Building Products truss designs have 1200 mm maximum batten spacing.
- Batten overhang using rouses 40 should not exceed 300 mm without Engineering approval.
- The tables have been determined based on the following assumptions:
 - batten is continuous over at least 3 spans;
 - all trusses are uniformly spaced;
 - fastener pullout loads determined for batten to Z chord connection.
- For sheet roof applications, batten connections to the chord of the first truss in from the gable end will require notching if the batten spacing is less than 1400 mm and the truss spacing is 450 mm. Strapping shall be 1.0 x 25 mm fastened to the web of the truss chord with 2 off 10 - 16 x 16 Hex. self-drilling screws.

ROOF CLADDING	BMT	SPAN TYPE	DESIGN WIND SPEED								
			W28			W33			W41		
			TRUSS SPACING			TRUSS SPACING			TRUSS SPACING		
CUSTOM ORB	0.42	END	600	900	1200	600	900	1200	600	900	1200
		INT	1200	1800	2400	1200	1800	2400	1200	1800	2400
		INT	1200*	1800*	2400*	1200*	1800*	2400*	1200*	1800*	2400*
	0.48	END	900	900	900	900	900	900	900	900	900
		INT	1200	1200	1200	1200	1200	1200	1200	1200	1200
		INT	1200*	1200*	1200*	1200*	1200*	1200*	1200*	1200*	1200*
CUSTOM BLUE ORB	0.60	END	900	900	900	900	900	900	900	900	900
		INT	1200	1200	1200	1200	1200	1200	1200	1200	1200
		INT	1800*	1800*	1800*	1800*	1800*	1800*	1800*	1800*	1800*
	0.81	END	1000	1000	1000	1000	1000	1000	1000	1000	1000
		INT	1300	1300	1300	1300	1300	1300	1300	1300	1300
		INT	1800*	1800*	1800*	1800*	1800*	1800*	1800*	1800*	1800*
TRIMDEK HI-TEN	0.42	END	1000	1000	1000	1000	1000	1000	1000	1000	1000
		INT	1700	1700	1700	1700	1700	1700	1700	1700	1700
		INT	1700	1700	1700	1700	1700	1700	1700	1700	1700
	0.48	END	1500	1500	1500	1500	1500	1500	1500	1500	1500
		INT	2100	2100	2100	2100	2100	2100	2100	2100	2100
		INT	2100	2100	2100	2100	2100	2100	2100	2100	2100
SPANDEK HI-TEN	0.42	END	1500	1500	1500	1500	1500	1500	1500	1500	1500
		INT	2100	2100	2100	2100	2100	2100	2100	2100	2100
		INT	2100	2100	2100	2100	2100	2100	2100	2100	2100
	0.48	END	1950	1950	1950	1950	1950	1950	1950	1950	1950
		INT	2800	2800	2800	2800	2800	2800	2800	2800	2800
		INT	2800	2800	2800	2800	2800	2800	2800	2800	2800
KLIP-LOK HI-TEN	0.42	END	1200	1200	1200	1200	1200	1200	1200	1200	1200
		INT	1800	1800	1800	1800	1800	1800	1800	1800	1800
		INT	1800	1800	1800	1800	1800	1800	1800	1800	1800
	0.48	END	1800	1800	1800	1800	1800	1800	1800	1800	1800
		INT	2300	2300	2300	2300	2300	2300	2300	2300	2300
		INT	2300	2300	2300	2300	2300	2300	2300	2300	2300
KLIP-LOK 700	0.42	END	1100	1100	1100	1100	1100	1100	N.R.	N.R.	N.R.
		INT	1800	1800	1800	1800	1800	1800	N.R.	N.R.	N.R.
		INT	1800	1800	1800	1800	1800	1800	N.R.	N.R.	N.R.
	0.48	END	1500	1500	1500	1500	1500	1500	1500	1500	1500
		INT	2100	2100	2100	2100	2100	2100	2100	2100	2100
		INT	2100	2100	2100	2100	2100	2100	2100	2100	2100

ROOF CLADDING	BMT	SPAN TYPE	DESIGN WIND SPEED								
			W30			W40			W50		
			TRUSS SPACING			TRUSS SPACING			TRUSS SPACING		
CUSTOM ORB	0.42	END	450	600	900	450	600	900	450	600	900
		INT	1200	1200	1440*	1080*	1080*	790*	810*	810*	710*
		INT	1200*	1200*	1440*	1080*	1080*	790*	1000*	1000*	710*
	0.48	END	600	600	600	600	600	600	600	600	600
		INT	1200	1200	1440*	1080*	1080*	790*	1000*	1000*	710*
		INT	1200*	1200*	1440*	1080*	1080*	790*	1000*	1000*	710*
CUSTOM BLUE ORB	0.60	END	900*	900*	900*	870*	870*	790*	645*	645*	645*
		INT	1200	1200	1440*	1080*	1080*	790*	910*	910*	710*
		INT	1460*	1460*	1140*	1275*	1180*	790*	1045*	1045*	710*
	0.81	END	1800*	1720*	1720*	1280*	1280*	790*	1265*	1150*	710*
		INT	1800*	1720*	1720*	1280*	1280*	790*	1265*	1150*	710*
		INT	1800*	1720*	1720*	1280*	1280*	790*	1265*	1150*	710*
TRIMDEK HI-TEN	0.42	END	1000	1000	1000	N.R.	N.R.	N.R.	N.R.	N.R.	N.R.
		INT	1405	1405	1140	1225	1180	790	1075	1075	710
		INT	1405	1405	1140	1225	1180	790	1075	1075	710
	0.48	END	1500#	1500#	1140#	1125#	1125#	790#	N.R.	N.R.	N.R.
		INT	1655#	1655#	1140#	1265#	1180#	790#	935#	935#	710#
		INT	1655#	1655#	1140#	1265#	1180#	790#	935#	935#	710#
SPANDEK HI-TEN	0.42	END	1145	1145	1140	N.R.	N.R.	N.R.	N.R.	N.R.	N.R.
		INT	1300	1300	1140	N.R.	N.R.	N.R.	N.R.	N.R.	N.R.
		INT	1300	1300	1140	N.R.	N.R.	N.R.	N.R.	N.R.	N.R.
	0.48	END	1350	1350	1140	1015	1015	790	N.R.	N.R.	N.R.
		INT	1625	1625	1140	1120	1120	790	N.R.	N.R.	N.R.
		INT	1625	1625	1140	1120	1120	790	N.R.	N.R.	N.R.
KLIP-LOK HI-TEN	0.42	END	1605	1605	1140	1350	1180	790	1330	1120	710
		INT	2080	2080	1140	1580	1180	790	1330	1120	710
		INT	2080	2080	1140	1580	1180	790	1330	1120	710
	0.48	END	N.R.	N.R.	N.R.	N.R.	N.R.	N.R.	N.R.	N.R.	N.R.
		INT	N.R.	N.R.	N.R.	N.R.	N.R.	N.R.	N.R.	N.R.	N.R.
		INT	N.R.	N.R.	N.R.	N.R.	N.R.	N.R.	N.R.	N.R.	N.R.
KLIP-LOK 700	0.42	END	N.R.	N.R.	N.R.	N.R.	N.R.	N.R.	N.R.	N.R.	N.R.
		INT	N.R.	N.R.	N.R.	N.R.	N.R.	N.R.	N.R.	N.R.	N.R.
		INT	N.R.	N.R.	N.R.	N.R.	N.R.	N.R.	N.R.	N.R.	N.R.
	0.48	END	N.R.	N.R.	N.R.	N.R.	N.R.	N.R.	N.R.	N.R.	N.R.
		INT	N.R.	N.R.	N.R.	N.R.	N.R.	N.R.	N.R.	N.R.	N.R.
		INT	N.R.	N.R.	N.R.	N.R.	N.R.	N.R.	N.R.	N.R.	N.R.

END = End Span INT = Internal Span * 5 fasteners per sheet # 4 fasteners per sheet N.R. Not Recommended

Appendix B

INSTRON Calibration

Table B1 INSTRON calibration

Calibration of INSTRON 100kN machine #1342-H1399

Material Laboratory

Calibration date 26/6/2003

Calibrated using Proving Ring
#116953

Range:- 0 - 10 kN

Deflection	Calculated Force (kN)	Indicated Force (kN)
14.70	1.00	1.00
29.37	1.99	2.00
44.43	3.01	3.00
59.00	4.00	4.00
73.70	5.00	5.00
88.07	5.97	6.00
102.77	6.96	7.00
117.53	7.96	8.00
131.97	8.94	9.00
146.87	9.95	10.00

Appendix C

Tensile Test Results

Table C1 Tensile test results

Sample No.	L_o (mm)	Width_{av} (mm)	F_{max} (kN)	L_{final} (mm)	Thickness_{av} (mm)	S_o (mm²)	R_m
BHP 1	49.87	12.48	6.26	54.13	0.77	9.61	651.16
BHP 2	50.03	12.46	6.20	54.93	0.77	9.55	649.54
BHP 3	50.18	12.60	6.29	53.55	0.79	9.96	631.91
BHP 4	49.89	12.57	6.25	54.5	0.77	9.68	645.96
BHP 5	50.08	12.58	6.29	54.71	0.77	9.64	652.42
Sample No.	L_o (mm)	Width_{av} (mm)	F_{max} (kN)	L_{final} (mm)	Thickness_{av} (mm)	S_o (mm²)	R_m
Stramit 1	49.51	12.43	6.35	53.84	0.78	9.74	651.60
Stramit 2	50.14	12.61	6.44	53.87	0.78	9.88	651.85
Stramit 3	50.25	12.59	6.45	54.87	0.78	9.86	654.08
Stramit 4	50.08	12.48	6.36	53.98	0.79	9.81	647.60
Stramit 5	49.9	12.61	6.43	53.23	0.79	10.00	643.14

Appendix D

Summary of Static Test Results

Table D1 BHP Static Trials

Test No.	Fastener type	Truss (metal/timber)	Load rate	Failure Load (kN)	Type of Failure	Comments
Trial 1	12 gauge x 40mm screw	timber	5 kN/min	6.22	Screw pulled out	Timber spilt when screw drilled into timber
Test 1	High tensile bolt with 1.45 mm thick washer	Metal	5 mm/min	12.8	Batten cracked through bolt hole	Thin washer used
Test 2	High tensile bolt with 1.45 mm thick washer	Metal	5 mm/min	7.92	Crack through bolt hole on one side and around washer on other side	Thin washer used
Test 3	High tensile bolt with 4.61mm thin washer	Metal	5 mm/min	6.00	Cracked around washer on both sides	Thick washer used with non-rounded edges
Test 4	Imperial high tensile bolt with 4.61mm thick washer	Metal	5 mm/min	5.82	Cracked around washer on both sides	Thick washer used with non-rounded edges
Test 5	Normal bolt with 4.61mm thick washer	Metal	5 mm/min	7.04	Cracked around washer on both sides	Thick washer used with non-rounded edges

Table D2 BHP Static Tests

Test No.	Fastener type	Truss (metal/timber)	Load rate	Failure Load (kN)	Type of Failure	Comments
Test 6	Imperial high tensile bolt with 4.61mm thick washer	Metal	5 mm/min	8.17	Cracked around washer on both sides	Thick washer used with rounded edges
Test 7	Imperial high tensile bolt with 4.61mm thick washer	Metal	5 mm/min	7.58	Cracked around washer on both sides	Thick washer used with rounded edges
Test 8	Imperial high tensile bolt with 4.61mm thick washer	Metal	5 mm/min	8.48	Cracked around washer on both sides	Thick washer used with rounded edges
Test 9	Imperial high tensile bolt with 4.61mm thick washer	Metal	5 mm/min	6.60	Cracked around washer on both sides	Thick washer used with rounded edges
Test 10	Imperial high tensile bolt with 4.61mm thick washer	Metal	5 mm/min	6.50	Cracked around washer on both sides	Thick washer used with rounded edges
Test 11	Imperial high tensile bolt with 4.61mm thick washer	Metal	5 mm/min	8.03	Cracked around washer on both sides	Thick washer used with rounded edges

Table D3 Stramit Static Trails

Test No.	Fastener type	Truss (metal/timber)	Load rate	Failure Load (kN)	Type of Failure	Comments
Trial 1	12 gauge x 40mm timber screws	timber MPG12	5 mm/min	8.05	Timber split through middle	Timber split all the way through the middle of the bolt holes before the batten of screws failed.
Trial 2	12 gauge x 40mm timber screws	timber MPG12	5 mm/min	7.63	Timber split through middle	Modified by screwing plates on the ends of the timber to see if gives better strength and to stop the timber from splitting before the batten fails.
Trial 3	12 gauge x 40mm timber screws	timber MPG12	5 mm/min	8.36	Timber split through middle	Used the same modified setup as test 2.

Table D4 Stramit Static Tests

Test No.	Fastener type	Truss (metal/timber)	Load rate	Failure Load (kN)	Type of Failure	Comments
Test 1	Imperial high tensile bolt with thick washer with round off edges	Metal	5 mm/min	9.78	Cracked batten around the washer	Failure identical on both sides
Test 2	Imperial high tensile bolt with thick washer with round off edges	Metal	5 mm/min	9.22	Cracked batten around the washer	Failure identical on both sides
Test 3	Imperial high tensile bolt with thick washer with round off edges	Metal	5 mm/min	8.32	Cracked batten around the washer	Different failure mode to test 1 & 2
Test 4	Imperial high tensile bolt with thick washer with round off edges	Metal	5 mm/min	8.60	Cracked batten around the washer	One side failed like test 1 & 2 and the other side failed like test 3
Test 5	Imperial high tensile bolt with thick washer with round off edges	Metal	5 mm/min	8.81	Cracked batten around the washer	Similar failure to test 3

Appendix E

Load vs. Displacement Curves for Static Tests

Table E1 Load vs. displacement curve for BHP static test 6

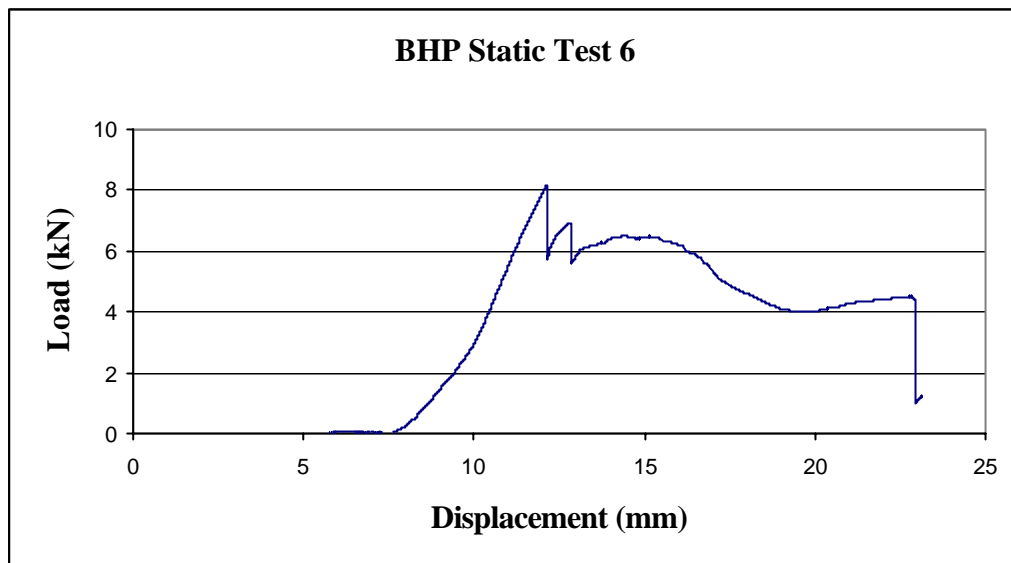


Table E2 Load vs. displacement curve for BHP static test 7

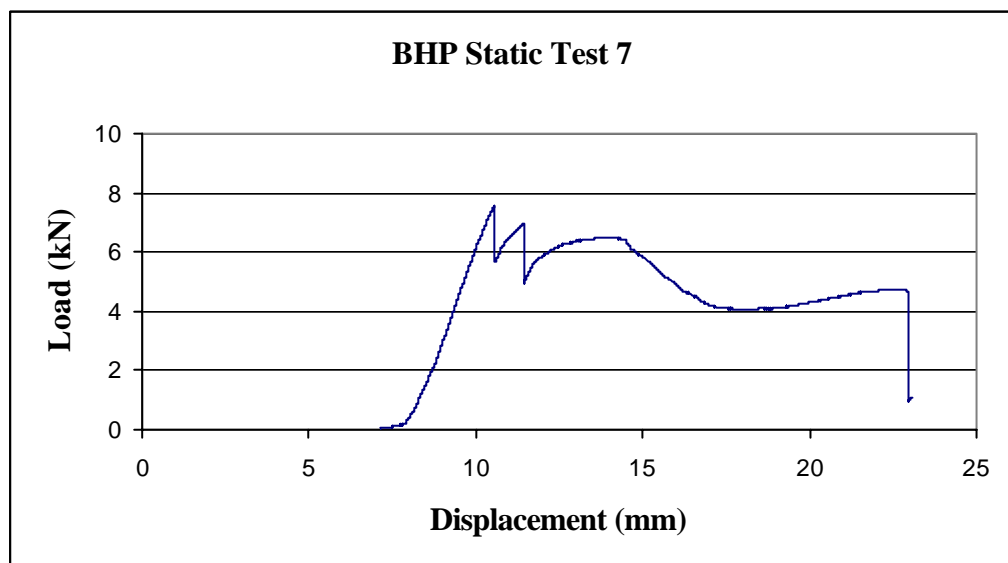
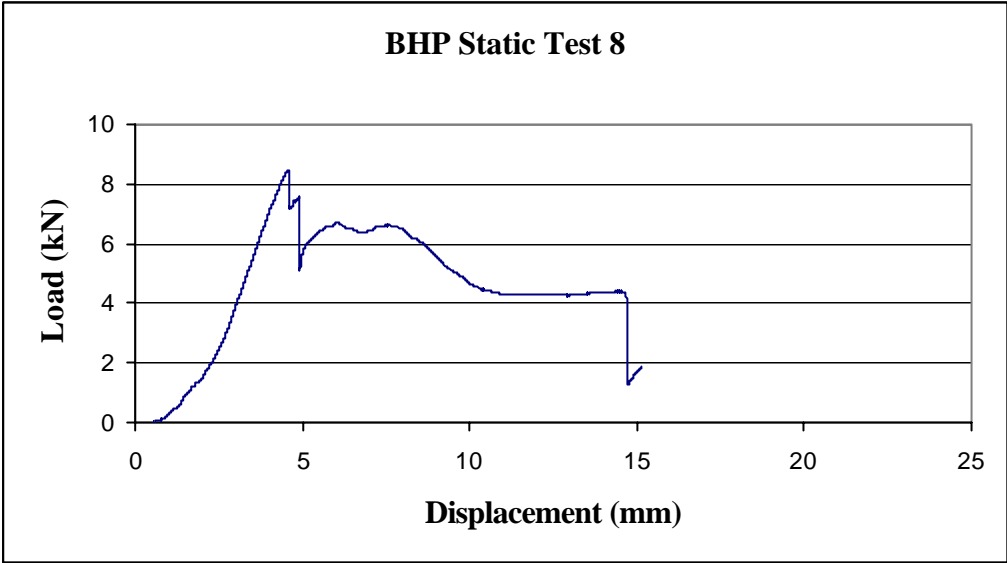


Table E3 Load vs. displacement curve for BHP static test 8



Note: Graph for BHP static test 9 is unavailable

Table E4 Load vs. displacement curve for BHP static test 10

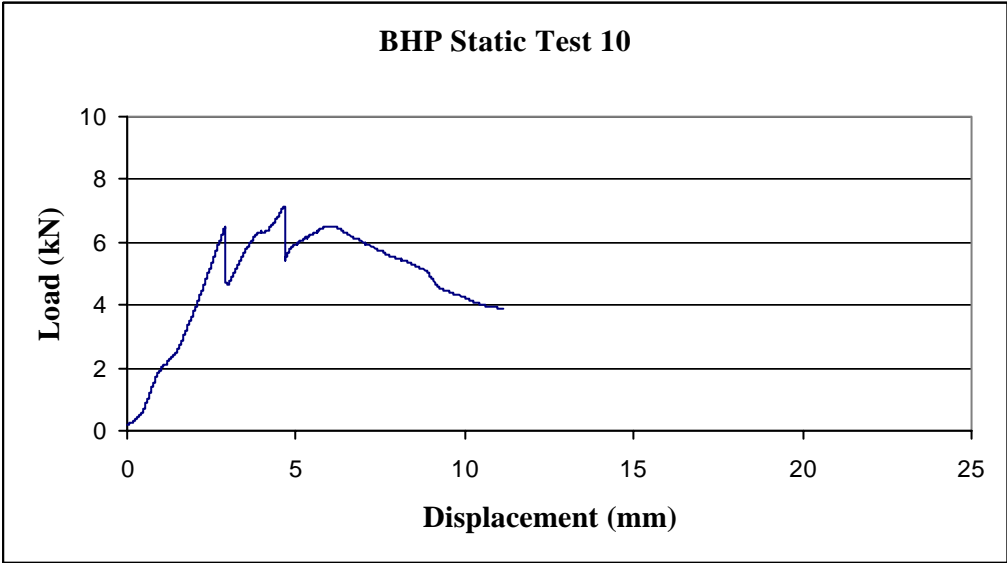


Table E5 Load vs. displacement curve for BHP static test 11

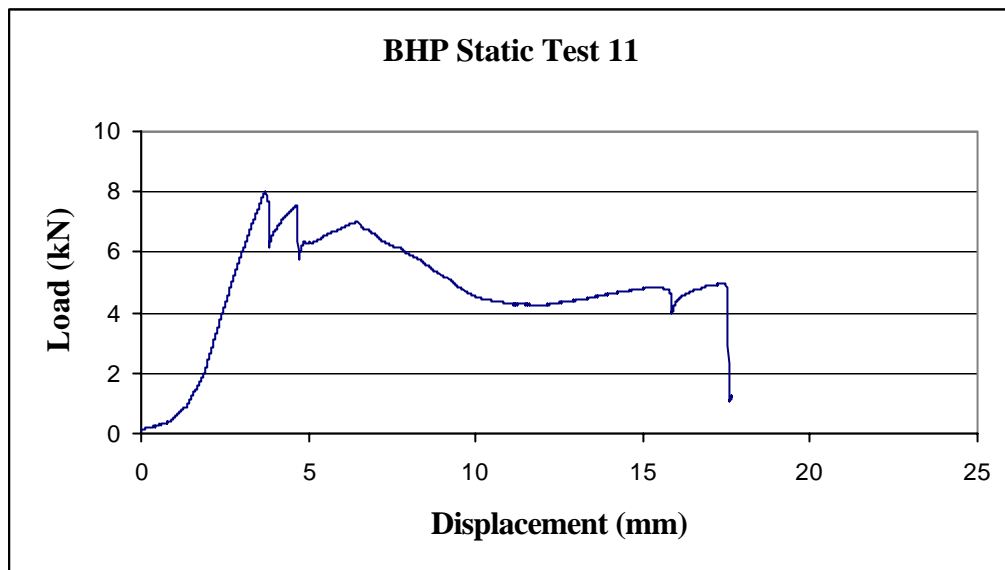


Table E6 Load vs. displacement for Stramit static test 1

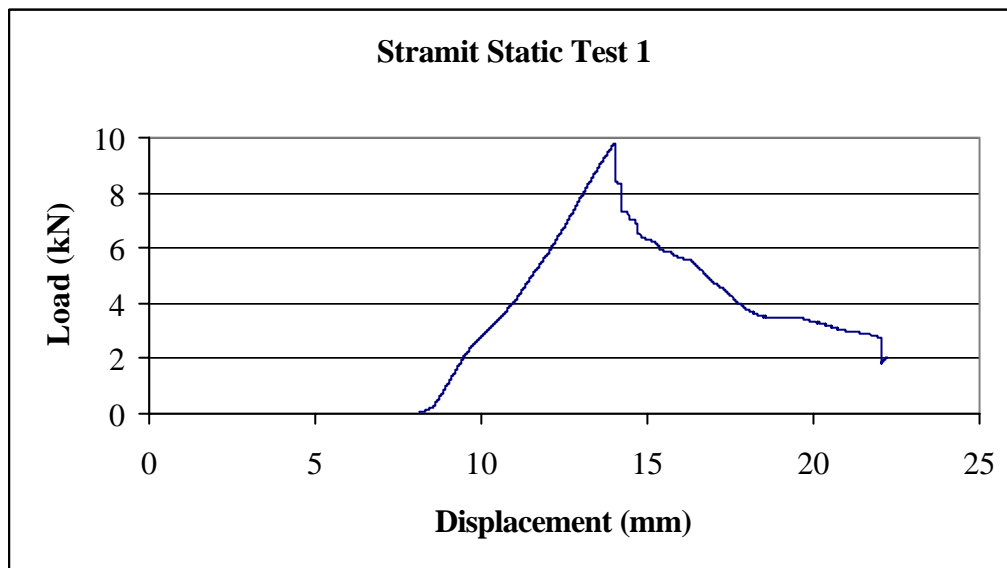


Table E7 Load vs. displacement curve for Stramit static test 2

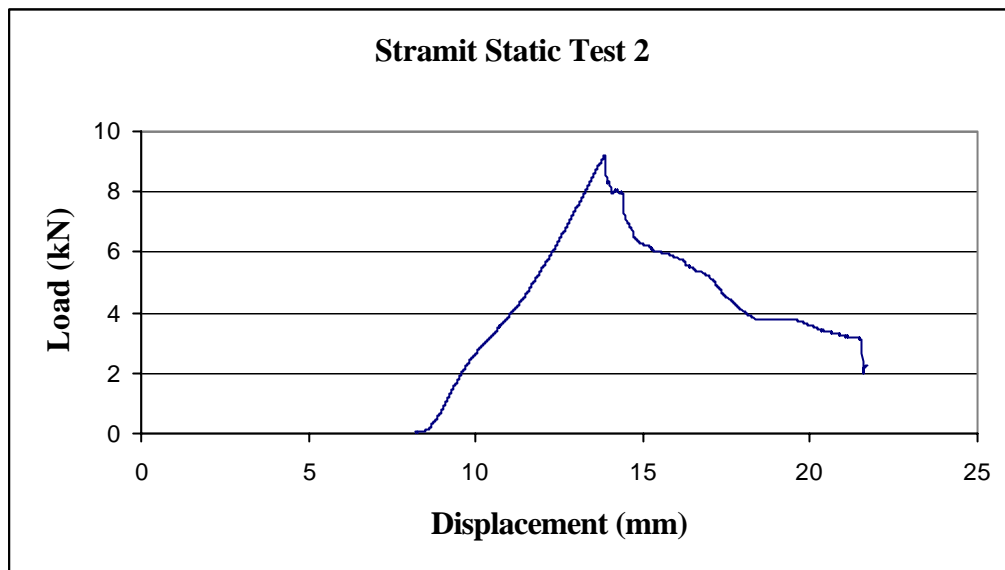


Table E8 Load vs. displacement curve for Stramit static test 3

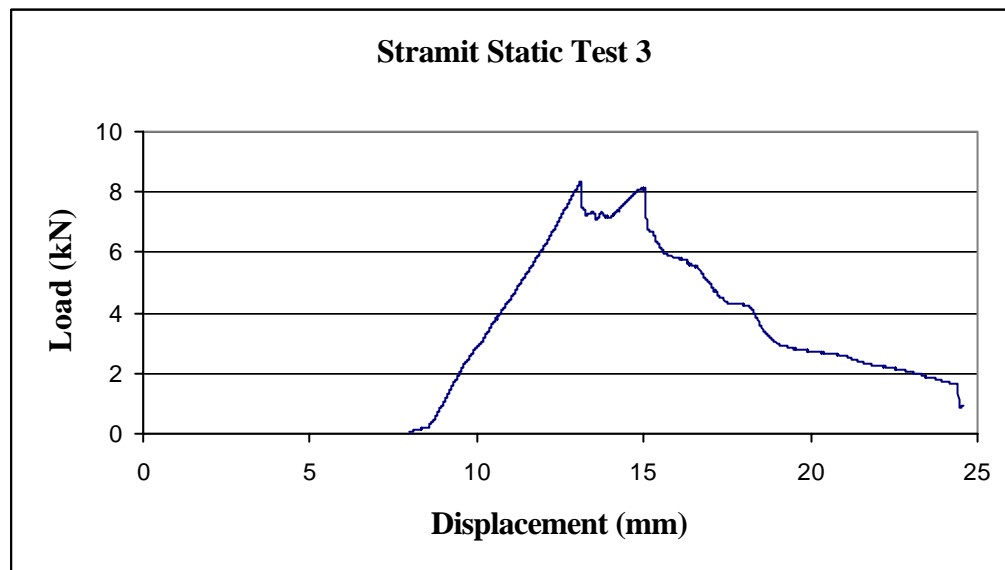


Table E9 Load vs. displacement for Stramit static test 4

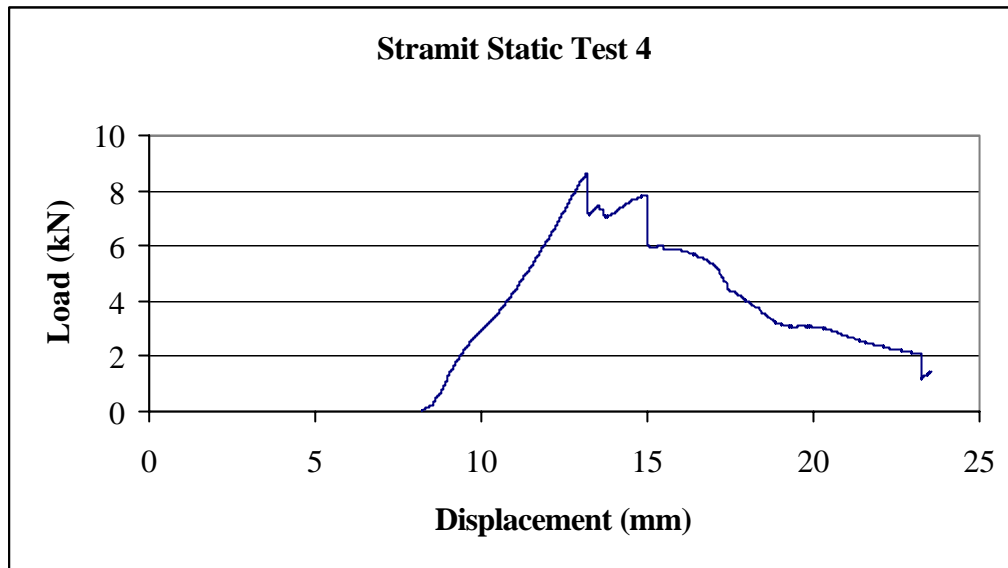
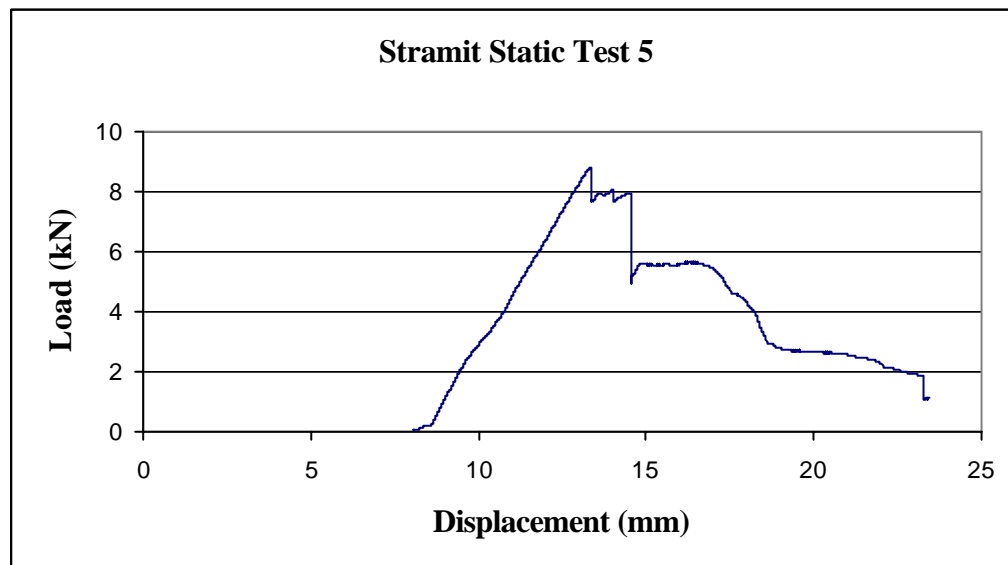


Table E10 Load vs. displacement for Stramit static test 5



Appendix F

Stramit Constant Amplitude Test Results

Table E1 Stramit constant amplitude cyclic test data

Test Number	Ramp	Amplitude	Frequency	Cycle bound (%)	Cyclic bound (kN)	No. of cycles till failure	>100 %	>90 %	>80 %	>70 %
2	3.6	3.6	0.8	80%	7.20	428	0	420	425	425
4	3.15	3.2	0.8	70%	6.30	677	97	670	672	674
5	3.6	3.6	0.8	80%	7.20	360	0	353	356	357
6	2.7	2.7	0.8	60%	5.40	1164	0	1155	1157	1160
7	2.25	2.25	0.8	50%	4.50	1562	0	1538	1556	1558
8	1.8	1.8	0.8	40%	3.60	3567	317	3231	3515	3521
16	3.8	3.83	0.8	85%	7.60	349	116	344	346	347
17	2.9	2.95	0.8	65%	5.80	718	326	707	716	717
18	2.45	2.5	0.8	55%	4.90	1353	834	1341	1348	1349
19	2	2.1	0.8	45%	4.00	2000	1063	1984	1992	1997
20	3.35	3.4	0.8	75%	6.70	436	346	429	433	433

Appendix G

Observed Crack Initiation and Propagation for 80% and 70% Constant Amplitude Cyclic Tests

Stramit Test 80% of the average static failure load (7.2kN)

1st lot of 100 cycles

- plastic deformation around the washer
- 5mm crack starting on underside of the batten at the web crease

2nd lot of 100 cycles

- BH1 - Approximately 7mm crack on underside of the battens and crack on topside approx 5mm along web crease
- BH2 – no observed crack on topside on batten still 5mm crack on underside

3rd lot of 100 cycles

- BH1 – approximately 14mm closed crack on topside of batten
- BH2 – no observed crack on topside of batten still 5mm crack on underside

4th lot of 100 cycles

- BH1 – open crack approximately 22mm long and open approximately 4-5mm in the centre of the crack
- BH2 – open crack approximately 15mm and open approximately 2mm

5th lot of 100 cycles

- Failed after 28 cycles

Stramit Test 70% of the average static failure load (6.3kN)

1st lot of 100 cycles

- Plastic deformation around the washer
- 5mm crack forming on the underside of the batten

2nd lot of 100 cycles

- no observed changes to cracks

- turned up edges buckling in around washer

3rd lot of 100 cycles

- BH1 – crack on underside of batten approximately 7mm
- BH2 – no observed changes

4th lot of 100 cycles

- BH1 – approximately 10mm crack on topside of batten
- BH2 – no observed changes

5th lot of 100 cycles

- BH1 – 15mm crack on topside of batten open approximately 0.5mm
- BH2 – no observes changes

6th lot of 100 cycles

- BH1 – approximately 20mm crack on topside along web crease, open approximately 3mm
- BH2 – approximately 15mm crack along web crease, open approximately 2mm

7th lot of 100 cycles

- Failed at 77 cycles into the block